Geological Quarterly, 2025, 69, 35
DOI: https://doi.org/10.7306/gq.1808

Contamination of Zn, Pb and Cd in topsoil in Katowice-Szopienice (southern Poland) as a result of 180 years of metal smelting: environmental implications

Jerzy CABAŁA[1, *], Weronika NADŁONEK[2], Martin NOVÁK[3] and Vladislav CHRASTNÝ[4]

[1] University of Silesia, Faculty of Natural Sciences, Będzińska 60, 41-200 Sosnowiec, Poland; ORCID: 0000-0002-2247-4827

[2] Polish Geological Institute – National Research Institute, Królowej Jadwigi 1, 41-200 Sosnowiec, Poland; ORCID: 0000-0002-2675-2601

[3] Czech Geological Survey, Department of Environmental Geochemistry and Biogeochemistry, Geologická 577/6, 152 00 Praha 5, Czech Republic; ORCID: 0000-0002-3450-1220

[4] Czech University of Life Sciences, Faculty of Environmental Sciences, Kamycka 129, 16500 Prague, Czech Republic; ORCID: 0000-0001-8383-1755

Cabała J., Nadłonek W., Novák M., Chrastný V., 2025. Contamination of Zn, Pb and Cd in topsoil in Katowice-Szopienice (southern Poland) as a result of 180 years of metal smelting: environmental implications. Geological Quarterly, **69**, 35; https://doi.org/10.7306/gq.1808

Associate Editor: Karol Zglinicki

The world's longest continuously operating Zn and Pb smelters were based in the Katowice-Szopienice area, for 180 years. In the current study, Scanning Electron Microscopy (SEM), Energy-Dispersive X-ray Spectroscopy (EDS), X-ray diffraction (XRD), and Atomic Absorption Spectroscopy (AAS) were used to examine recently collected topsoil samples from 0–10 cm depth. AAS studies revealed extremely high concentrations of heavy metals in the topsoil. Zinc, Pb, and Cd concentrations exceeded 10,000, 4,650 and 204 mg kg^{-1}, respectively. The metals are mostly derived from sulphides, oxidized Zn-Pb ores, smelter slags, and emissions from metallurgical processes, such as metal alloy production. The abundance of each group of minerals depends on the type of industrial activity in the area (Zn or Pb metallurgy, metal rolling mills, smelter waste dumps, etc.). Sources of potentially toxic Pb, Cd, As and Sb are primary and secondary mineral assemblages. The largest part of Zn and Pb is bound in minerals that are products of base-metal ore weathering and in synthetic silicate minerals formed during Zn smelting. Smithsonite, hemimorphite and cerussite are among the most common secondary minerals. Metals from carbonate and silicate minerals are mobilized more slowly. Leaching tests showed that there is a risk of transfer of toxic Cd ions into soil solutions (>20% of Cd is present in the ion-exchange fraction). Our study will be useful for planning reclamation and revitalization efforts aimed at minimizing the adverse impact of metal-bearing minerals on the environment.

Key words: zinc lead, cadmium, topsoil pollution, heavy metal leaching, historical Zn-Pb smelting.

INTRODUCTION

Zinc mining and metallurgy in Europe started in the mid-18th century when William Champion developed a metallurgical technology for Zn production in Bristol, England (Dungworth and White, 2021). Large-scale Zn production began in the early 19th century. Its price and the profitability of production increased rapidly. The profits made from Zn production were much higher than those from coal or Fe ore mining. In the 19th century and early 20th century, the largest centres of Zn production were Belgium (Neutral Moresnet, Wallonia), the USA (New Jersey, Illinois, Missouri), and Germany (Ruhr and Upper Silesia). Gradual depletion of European Zn-Pb ore resources was accompanied by increasing Zn production in Asia (China, India), South America (Peru, Bolivia), Australia and North America (USA, Mexico, Canada). In 2021, global annual Zn production exceeded 13 million tonnes (USGS, 2022).

Zinc is geochemically related to Pb. Under similar conditions, ores of these metals form sediment-hosted deposits, among which the most important are Mississippi Valley (MVT) and Sedimentary Exhalative (SEDEX) types (Leach et al., 2010). The geochemical similarity between Zn and Cd ions results in accumulation of significant amounts of Cd and Tl in Zn minerals (Viets et al., 1996; Mikulski et al., 2020). Zn-Pb ores

---

* Corresponding author, e-mail: jerzy.cabala@us.edu.pl

Received: March 20, 2025; accepted: September 1, 2025; first published online: October 17, 2025

commonly have high concentrations of Ag, Cu, As and Sb (Cabala, 2001; Cabala and Teper, 2007). Therefore, soils, water and air in Zn mining and smelting areas are contaminated with these potentially toxic elements (PTEs). Breaches of accepted standards, often involving extreme concentrations of highly toxic Pb, Cd and Tl, have been reported in many areas of the world (Stafilov et al., 2010; Li et al., 2015; Kicińska, 2020; Pasieczna et al., 2020: Rahmanov et al., 2021; Soto-Jiménez et al., 2023). In soils, Zn or Pb concentrations commonly exceed 10,000 mg kg^{-1} and Cd concentrations commonly exceed 500 mg kg^{-1} (Cabala et al., 2008; Rahmonov et al., 2021; Nadłonek et al., 2024).

We studied the topsoil at Katowice Szopienice (Upper Silesia, Poland), the site of the longest continuously operating large-scale Zn smelter in the world, active from 1834 to 2008 (Gorecki, 2018). Previous studies have focused on the mineral composition and geochemistry of the smelter slags (Kierczak et al., 2010; Tyszka et al., 2014, 2018; Rożek et al., 2015; Cabala et al., 2020) but there is much less information on the potential leaching of PTEs from soils affected by metallurgy. There is also little data on mineral phases and concentrations of Pb, Zn, Cd, Cu, Tl, As and Sb in soils, bottom sediments and wastes. Identification of mineral phases and PTE concentrations is important for understanding the geochemical transformations of metal-bearing mineral phases over long periods of time and for assessing potential health risks to humans and animals. Studies of these variables can assist in the redevelopment of affected sites and in assessing the effectiveness of previous redevelopment work to reduce PTE concentrations. A lack of information on metalliferous mineral phases and the leaching potential of PTEs in areas affected by Zn-Pb smelting can lead to environmental pollution being either overlooked or exaggerated in local public consciousness.

HISTORY OF ZINC PRODUCTION IN KATOWICE-SZOPIENICE

The history of large-scale Zn and Cd production in the the Silesian-Kraków region (southern Poland) is of >200 years duration. Lead and Ag mining in the area began as early as in the 12th century (Cabała et al., 2020). The region abounds in shallow-depth Zn-Pb ores. A significant increase in Zn production from the Zn-Pb deposits of Upper Silesia was possible thanks to the use of horizontal retorts, developed by Ruberg in 1798 (Anyadike, 2002). This technology, called the 'Silesian method', significantly increased the profitability of Zn production (Krantz, 1911). In the first decades of the 19th century, numerous mines were opened in Upper Silesia, exploiting Zn-Pb ores from supergene deposits. Locally, in shallow zones of weathered primary Zn-Pb sulphide deposits, there are also oxidised zinc ores, named "galman" in Polish mining terminology. Two types of galman were recognized (Coppola et al., 2009; Mikulski et al., 2020). The first is a highly ferruginous red galman containing hydrous iron oxides (mainly goethite), smithsonite, and hemimorphite; and the second one, white galman (not very common), is enriched in Fe-smithsonite and Zn-dolomite. They represent ores in which most of the zinc and lead minerals are bound in carbonate minerals (smithsonite, monheimite, hydrocynkite, cerussite) and silicates (hemimorphite). The term "calamine" was also used for non-sulphide Zn-Pb deposits. In the late 19th century, deeper Zn-Pb sulphide ores started to be mined, making the region one of the world's largest Zn and Pb producers (Krantz, 1911).

At the beginning of the 19th century, investments in Zn-Pb ore mining and Zn production were made by (among others) Karol Godula (19 galman mines, 3 Zn smelters), Bergwerksgesellschaft Georg von Giesches Erben (2 Zn-Pb mines, 5 Zn and Pb smelters), Hohenlohe Werke A.G. (3 Zn smelters), the Kingdom of Prussia (3 Zn smelters and one Pb smelter), the Polish Government and the Franco-Russian Society (3 Zn smelters and 6 galman mines), and the Austro-Hungarian Government (2 Zn smelters, 4 galman mines) (Hartshorne, 1934; Gorecki, 2018).

In 1910, 23 Zn-Pb ore mines were in operation in Upper Silesia; 195,000 tonnes of oxidised, smithsonite-type ore, 402,000 tonnes of sulphide ore, 58,000 tonnes of Pb ore and 8,000 tonnes of pyrite were mined (Hahn, 1910). Zinc production in Upper Silesia in 1910 was about 138,000 tonnes, with 6 smelters in operation. The Szopienice smelter produced 30,480 tonnes of Zn (Krantz, 1911). In 1910, Upper Silesia's share of world Zn production was 17.2%. Only the USA (30.7%) and Belgium (21.1%) had larger shares of the market. Sizeable Zn production took place in Szopienice in smelters owned by Bergwerksgesellschaft Georg von Giesches Erben. The largest of these was the Wilhelmina Zn works (operational from 1834). The investments of the Giesche concern were concentrated in the area of Szopienice and the neighbouring villages. The 'Paul' Zn smelter was expanded in 1861, the 'Walter Croneck' Pb smelter was opened in 1864, the 'Norma' smelter began operation in 1880 and the 'Bernhardi' smelter was opened in 1887. In the neighbourhood of the Bernhardi ironworks, a Zn rolling mill was built in 1904 and operated until 2002. Close to the 'Wihelmina' smelter, the modern 'Uthemann' Zn smelter and the 'Sager' Zn blende roasting plant were built in 1912 (Fig. 1).

From 1912 to 1931, the Szopienice smelter was one of the most modern in the world, with an annual Zn production of 25,000 tonnes. In the 1920s and 1930s, the production of Zn, Pb, Cd and Ag in Upper Silesia increased significantly as a result of consolidation of German, Franco-Belgian, Anglo-American and Polish capital. After the Second World War, the infrastructure of the Szopienice smelters served for the production of Cu and Ag in addition to Zn, Pb and Cd. From 1973 onwards, the production of rolled products made from Cu and its alloys began. In 2008, the Szopienice non-ferrous metals smelter was closed.

HEALTH RISKS OF Pb EMISSIONS

Scientific studies clearly show a correlation between elevated Pb concentrations in humans and Pb or Zn smelting (Gzyl, 1997; Soto-Jimenez and Flegal, 2011; Zhang et al., 2012; Li et al., 2015; Charkiewicz and Backstrand, 2020; Zhou et al., 2022; Raj and Das, 2023). The strong toxic effects of Pb released in smelting processes have been recognized since the 19th century. The residents of Liege (Belgium), where a Zn smelter of the Société Vieille Montagne operated until the 1880s, were particularly strongly affected by Pb emissions. The plant's emissions of toxic Pb compounds in an urban area (Saint-Léonard) contributed to its closure in 1880 (Péters, 2016). During the same time period in Upper Silesia (southern Poland), the smelters of the Bergwerksgesellschaft Georg von Giesches Erben (Szopienice) and Hohenlohe Werke A.G. (Katowice Wełnowiec) operated continuously, despite the impact of their emissions on urban areas.

Lead poisoning related to the smelter technology in Upper Silesia was described by Hamilton (1914), who reported a high

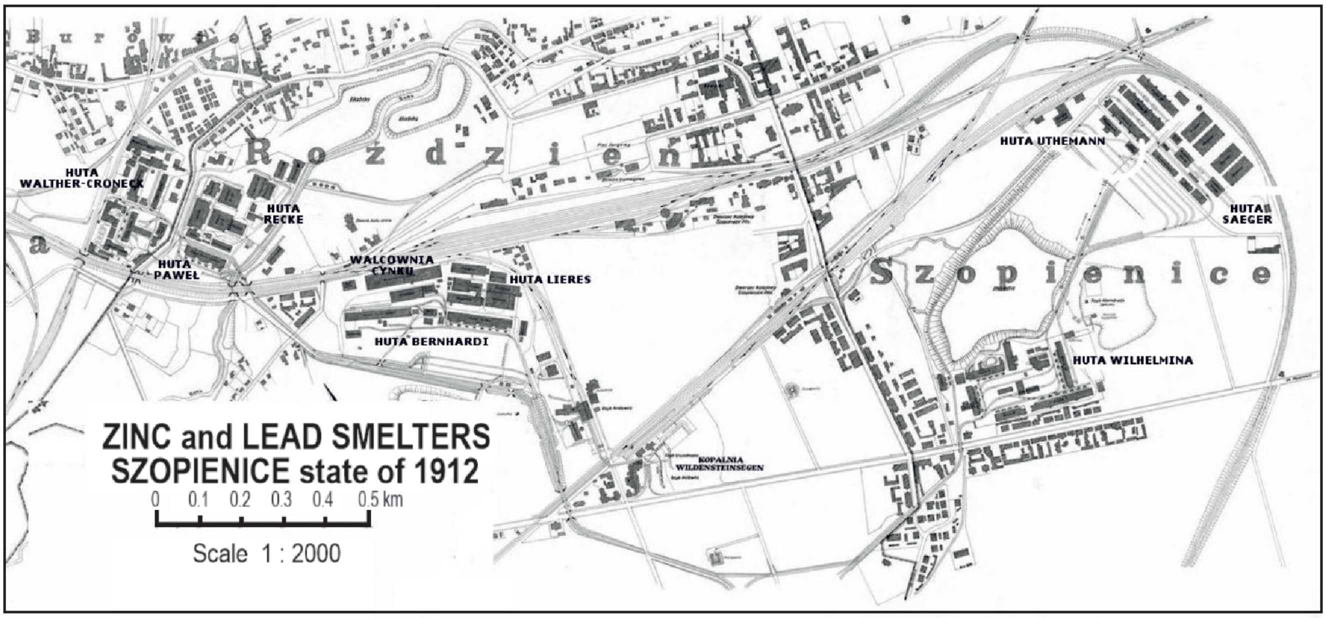

Fig. 1. The complex of Zn and Pb smelters in Szopienice

Infrastructure from 1912; https://szopienice.pl/2012/08/24/o-szopienickim-hutnictwie-slow-kilka/ with additions

level of Pb sickness among the workers at the Royal Smelter in Strzybnica (Royal Friedrichshutte in Tarnowitz) and the Walter Croneck smelter in Katowice-Szopienice. Uncontrolled Pb emissions at the Walter Croneck smelter in Szopienice were high, as indicated by the very high rate of Pb poisoning (up to 68%) among workers between 1903 and 1905 (Neisser, 1907).

Submicroscopic, metal-containing particles of the respirable fraction pose a direct threat to human health, particularly that of children (Osman et al., 1992; Dalton and Bates, 2005; Charkiewicz and Backstrand, 2020). Lead poisoning in children as a function of their distance from the Zn smelter in Szopienice was studied by Osman et al. (1992). Smelter emissions also have a significant impact on Pb and Cd concentrations in soils (Zhou et al., 2022). The mobility of metals from phases originating from mining and processing of metal ores results in their transfer to edible plants (Liu et al., 2005). Studies in the Silesian-Kraków region indicate that Zn, Pb and Cd are transferred from contaminated topsoil to plants, posing a real risk to human health (Ćwieląg-Drabek et al., 2020).

The large scale and long duration (>180 years) of the metallurgical production of Zn, Pb and Cd in this region has led to a perception in the public mind the that local environment is extremely polluted with heavy metals, particularly Pb.

Although Pb poisoning was a growing problem throughout the mid-20th century, it was not until the 1970s that medical research carried out in Szopienice Wadowska-Król and Hager-Małecka clearly identified widespread Pb poisoning in children living in the vicinity of the smelter (Jędryka, 2020; Cabała et al., 2021).

MATERIALS AND METHODS

SAMPLING

Forty samples each weighing ~1 kg were taken from the topsoil layer (0–10 cm) from an area of ~0.25 m^2 each. The samples, with an irregular distribution, were collected in the Katowice-Szopienice area. Several samples were taken from Areas 1–5 (Fig. 2). Samples were collected in areas where the land surface has not been redeveloped and rehabilitated in the last few decades. The sampling was performed in areas differing in historic or current land use, and distance from the largest smelter in Area 1 (Table 1). Individual sampling sites were selected so that a preliminary assessment of the type of metalliferous mineral phases and element concentrations in topsoil could be made both in the former smelter areas, and in adjacent areas. The very high degree of industrialization and urbanization in the former Szopienice smelting area make it difficult to obtain samples of soils contaminated by the historical smelting.

Samples from Areas 1, 2, and 3 represent soils from different periods of metallurgical activity. These soils cannot be distinguished by horizons resulting from soil-forming processes, and often lack a humus layer. After the end of metallurgical activity in the 1980s, the historic zinc smelter buildings were demolished, leaving only a few historic buildings and a water tower. Currently, Areas 2 and 3 are built up with new industrial buildings, service and administrative offices, as well as asphalt and concrete roads. Samples from Areas 4 and 5 represent

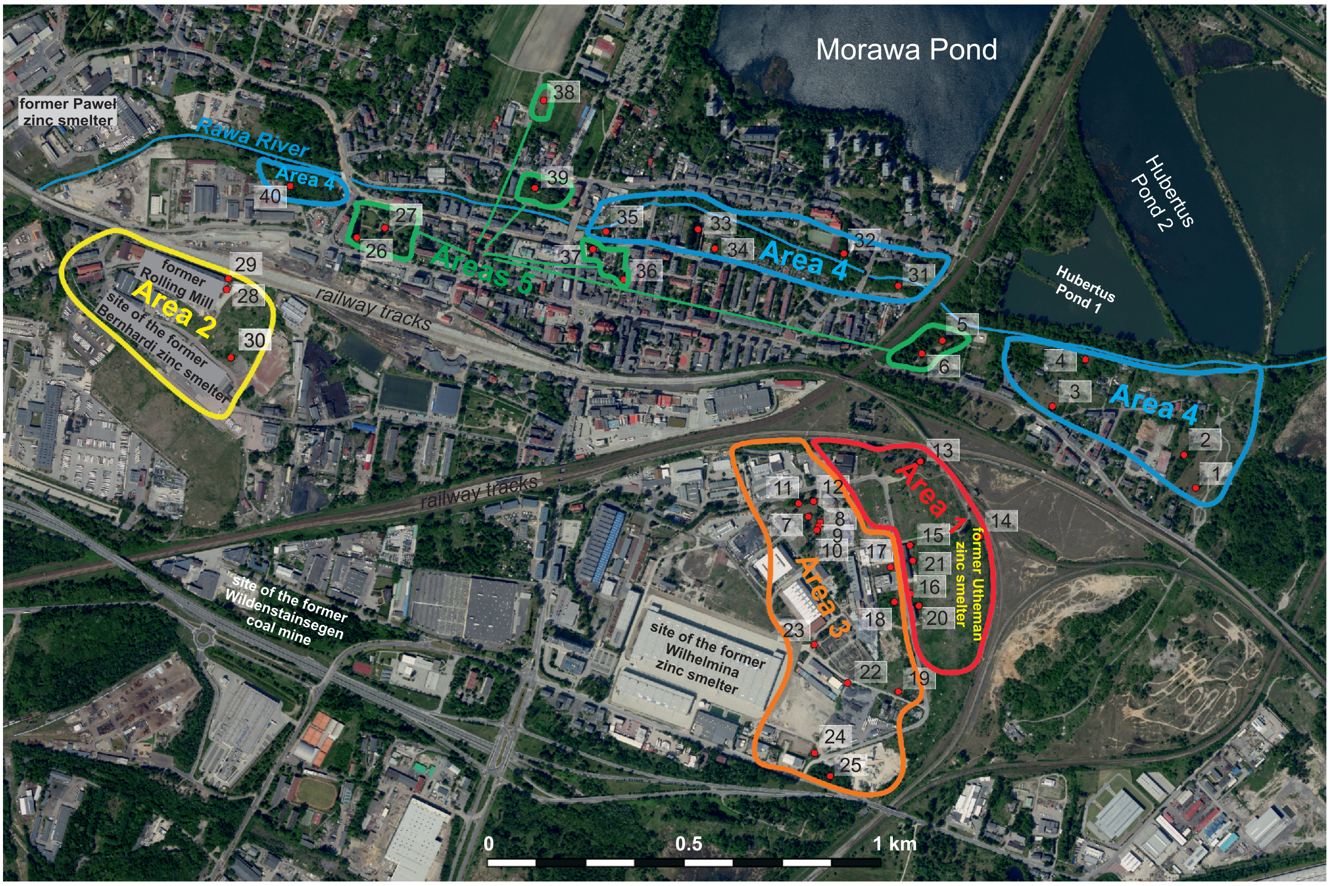

Fig. 2. Map of the study area in Katowice-Szopienice with locations of the sampling sites

Area 1 – area of the former Uthemann zinc smelter; Area 2 – area of the former Rolling Mill and the Bernhardi zinc smelter; Area 3 – areas west of the former Uthemann zinc smelter; Area 4 – along the River Rawa, to the N and NE of the former Uthemann zinc smelter; Area 5 – urban square areas and childrens' playgrounds; map sources: Airbus, CNES / Airbus, Maxar Technologies, Map data 2025 Google

technosols and sandy soils with low humus content. Industrial soils, classified as technosols, are soils that have been altered from their natural state as a result of human industrial activity. They are classified in The World Reference Base for Soil Resources (Rossiter, 2007). The soil structure and mineral composition have been altered, and heavy metals, chemicals and hydrocarbons have been introduced into the topsoil. Samples from Area 5 come from park areas, town squares and playgrounds. Only sample nos. 38 and 39 are brown-type soils that have been used agriculturally in the past.

SCANNING MICROSCOPY WITH ENERGY DISPERELECTRON SIVE SPECTROSCOP

Backscattered-Electron (BSE) Images and Energy Dispersive Spectroscopy (EDS) analyses were conducted with a Thermo Scientific Quanta 250 scanning electron microscope (SEM) equipped with a 4-quadrant BSE semiconductor detector and an UltraDry EDS detector. Operating conditions were under a high vacuum and with a 15kV accelerating voltage. The topsoil samples were sieved and the <0.2 mm fractions were prepared for SEM imaging and EDS microanalyses. Samples were fixed on aluminum stubs with double-sided carbon tape. 110 SEM slides from topsoil samples were analysed. BSE images (210) and EDS microanalyses (220) of topsoil samples were made. Submicroscopic studies were carried out in the Microscopic Research Laboratory at the Faculty of Natural Sciences of the University of Silesia in Katowice.

ICP-ES/MS

The samples were first crushed using a jaw crusher and pulverized in an agate ball mill. The material was then quartered before major and trace element analysis. Approximately 0.25 g of each sample was digested using the four-acid method (HF + $HClO_4$ + HCl + HNO_3) with the use of thermal conductivity. Elements in these solutions were analysed by ICP-ES (emission spectrometry with excitation in an induced plasma) or ICP-MS (inductively coupled plasma mass spectrometry) depending on the concentration of elements in the samples.

ICP-ES analyses were performed by Bureau Veritas Commodities Canada Ltd. using the MA250 analytical procedure. This methodology was chosen because of the low lower limits (in mg kg^{-1}) of quantification of, e.g., Cu (0.1), As (0.2), Cd (0.02), Sb (0.02), Tl (0.05) and Ag (20 ppb), however, the upper limit of quantification for Pb and Zn is high (10,000 mg kg^{-1}). The results are given in Appendix 1.

Table 1

Metal-bearing minerals in the topsoil around the historic zinc smelter in Katowice-Szopienice (data from XRD and SEM/EDS studies)

Site no	Mineral phases			
	Barren phase	Major metalliferous phase	Minor phase	Accessory minerals
Area 1. The area of the former Uthemann zinc smelter	quartz (++++) diopside (++) K,Na aluminosilicate* (++) orthoclase (++)	hemimorphite (+++) sphalerite (++) Zn carbonate* (++) hematite (++) Pb sulphide* (+) Pb carbonate* (++) goethite (++) pyromorphite (++) Fe sulphide* (++) osakaite (+)	barite* (++) Ca-Al silicate with Zn* (++) Fe oxide with Zn* (++) wurtzite Fe-Mn oxide with Zn* (+) Zn sulphide with Cd* (+) Fe-Zn oxide* (+) Zn-Pb-Mn oxide* (+) Zn-Pb oxide with As* (+) Ca-Zn aluminosilicate* (+) Fe-Zn sulphate* (+)	zircon* (+) Ca-Mg silicate (asbestos)*(+) Fe metallic* (+) Ce-Nd phosphate* (+) Cu-Sn alloy* (+) Ni-Ta-Ti-Cr-Co alloy* (+) Ni metallic* (+) aluminosilicate with Mo,Zn*(+) srebrodolskite (++)
Area 2. The area of the former Rolling Mill and the Bernhardi zinc smelter	quartz (++++), dolomite (+++), albite (++), microcline (++), muscovite (++) kaolinite (++), mullite (+) calcite(+)	Pb carbonate* (++) Fe-Mn oxide* (++) Zn carbonate* (+) Fe-Zn carbonate* (+)	barite* (++) Fe-Zn oxide* (+) Fe-Ca silicate with Pb*(+)	Pb metallic* (++) Pb-Sb; Pb-Sb-Sn alloy* (+) Sn oxide* (+) Fe-Ti oxide* (+) Mn oxide with Zn,Pb,Cu*(+) Fe oxide with Zn,Pb* (+)
Area 3. Industrial area west of the former Uthemann zinc smelter	quartz (+++) Fe-aluminosilicate*(++) mullite (+) kaolinite (+) orthoclase (+)	Pb carbonate* (++) Fe oxide* (++) Fe sulphide* (+) pyromorphite Willemite	gypsum (++) barite* (+) Pb sulphide* (+) Zn sulphide* (+) Fe-Mn oxide with P* (+) Zn carbonate* (+)	Fe-Cr alloy* (+) Fe-Ti oxide* (+)
Area 4. Areas along the River Rawa, to the N and NE of the former Uthemann zinc smelter	quartz (++++), albite (+), microcline (++), kaolinite (+), Ca,Fe aluminosilicate* (+)	Zn oxide* (++) Fe oxide (++) Zn sulphide* (+) Zn,Ca,Fe silicate* (+) aluminosilicate with Fe,Mn,Ti oxide* (+)	barite* (++) Fe oxide with Zn* (+) Fe sulphide* (+) Fe oxide with Pb, P* (+) Zn oxide with Cd* (+) Zn oxide with Cu* (+) Cr oxide with S, Zn* (+)	zircon* (++) Ce,Nd,Pr phosphate* (+) Fe-Cr alloy* (+)
Area 5. Urban square areas and childrens' playgrounds	quartz (++++), aluminosilicates* (+++) dolomite (++)	Fe oxide* (++) Fe-Mn oxide* (++) Mn oxide with Zn* (+) K-aluminosilicate with Zn* (+) gypsum* (+) Fe aluminosilicate* (+)	Zn sulphide* (+) barite* (+) Pb sulphide* (+) Pb carbonate* (+) Zn carbonate* (+)	Ce-La phosphate* (+) zircon* (+)

* – data from SEM/EDS studies; frequency of occurrence based on mineral grains counted in 1 cm^2 of SEM preparation: + – one grain, ++ – 2–3 grains, +++ – 3–10 grains, ++++ – >10 grains

X-RAY DIFFRACTION

X-ray powder diffraction data were obtained using a PANalytical X'PERT PRO–PW 3040/60 diffractometer (Malvern Panalytical Ltd, Malvern, UK) (CuK_1 source radiation, Ni-filter to reduce the K_ radiation, and X'Celerator detector). Quantitative data processing was performed by means of the X'PERT High Score Plus software using the latest PDF4+ database. The research was carried out at the X-ray Structural Research Laboratory at the Faculty of Natural Sciences of the University of Silesia in Katowice.

METAL LEACHING TEST

Six topsoil samples were selected for metal leaching studies. All represented high levels of heavy metal contamination. Three samples (SZ 7, SZ 11 and SZ 22) were taken in Area 2, adjacent to the former Zn smelter. This area was used as a logistical base for the smelter and was thus most exposed to metal deposition. The other three samples (SZ 14, SZ 29 and SZ 33) were from Areas 1, 2 and 4 respectively. Sequential extraction separated particulate trace metals (Zn, Pb, Cd, Cu, As, Sb) into five fractions: exchangeable (F1), carbonate-bound

Table 2

Element concentrations means in mg kg^{-1} and standard deviation

Site no.	Pb*	Zn**	Cd	Tl	As	Sb	As/Pb	Sb/Pb	Cd/Pb
Area 1. The area of the former Uthemann zinc smelter	2563 (2821)	8992 (2850)	204 (244)	3.4 (1.6)	96 (80)	13 (14)	51 (31)	6 (3)	49 (17)
Area 2. The area of the former Rolling Mill and the Bernhardi zinc smelter	4695 (1607)	10000 (9000)	197 (109)	15 (5)	229 (129)	61 (35)	50 (19)	13 (4)	41 (14)
Area 3. Areas west of the former Uthemann zinc smelter	4006 (3647)	8474 (3090)	79 (58)	2 (1.8)	414 (341)	27 (44)	121 (43)	5 (4)	31 (20)
Area 4. Along the River Rawa, to the N and NE of the former Uthemann zinc smelter	737 (519)	3599 (2124)	28 (13)	2 (1.7)	50 (57)	6 (4.4)	61 (27)	10 (4)	48 (20)
Area 5. Urban square area and playgrounds	1147 (902)	2789 (1722)	26 (16)	1.7 (1)	42 (914)	16 (13)	60 (37)	17 (14)	33 (28)
Kimbrough and Cardner (1999) (data from secondary lead smelter)							8.1	20.4	1.4
Eckel et al. (2002) (data from lead smelter in USA)	RANGE MEDIAN						8.5 –1200 54	1.6–34 12	0.7–26 13

* – Pb in two samples from Area 3 was determined at the upper limit (10,000 mg kg^{-1}) for the MA250 procedure; its actual average content was higher, **– Zn in 19 samples from Areas 1, 2, 3 was determined at the upper limit (10,000 mg kg^{-1}) for the MA250 procedure; its actual average content was higher; As, Sb and Cd ratios normalized to Pb = 1000

(F2), Fe-Mn oxide-bound (F3), organic matter-bound (F4) and residual (F5) (Tessier et al., 1979). Solution analyses were performed by ICP-ES. Extraction methods are divided into several steps. A tabular summary of the Tessier et al. (1979) sequential extraction procedure is given in Appendix 2. Leaching tests were performed at the Laboratory of the Central Mining Institute – National Research Institute, Katowice, Poland.

RESULTS

In the study area, minerals containing Zn, Pb, Fe, Cd, As, Sb, Cu and Ba are abundantly present in the topsoil (Table 1). Consequently, high or very high levels of concentrations of potentially toxic metals (e.g., Pb, Zn, Cd, Tl) and metalloids (As, Sb) are present in the soil (Table 2). Concentrations of Mo, Ni, Co, Mn, U, Th, Sr, Bi, V, Ca, P, La, Cr, Mg, Ti, Al, Na, K, W, Zr, Be, Sc, Y, Ce, Pr, Nd, Sm, Eu, Gd, Tb, Dy, Ho, Er, Tm, Yb, Lu, Hf, Li, Rb, Ta, Nb, Cs, Ga, In, Re, Se and Te did not differ significantly from their average levels in the soils of southern Poland (Kabata-Pendias and Pendias, 1999).

XRD ANALYSIS OF MINERAL COMPONENTS

XRD studies have shown that Zn-rich and Fe-rich minerals make up a significant proportion of all topsoils throughout the study area (Fig. 2). The amounts of these minerals are particularly high in Areas 1 and 3.

The topsoil in the former smelter area is characterized by significant proportions of hemimorphite ($Zn_4[(OH)_2/Si2O_7]$ H_2O) (~8.7%) and sphalerite (ZnS) (~3.7%). Wurtzite, a high-temperature hexagonal phase of ZnS, was also identified (Fig. 3A). Of the Zn-bearing minerals, osakaite [$Zn_4(SO_4)(OH)_6{\cdot}5H_2O$] was recognized (Fig. 3A).

Around the former smelter, the proportion of metal-bearing minerals in the topsoil was different, with the characteristic occurrence of mullite (5%), cristobalite low (0.3%), gypsum (1.2%), hematite (0.7%), willemite (0.4%) and pyromorphite (0.1%) (Fig. 3B).

In Area 2 no phases with Zn, Pb, Fe, As or Sb were identified by XRD. A high (~21.3%) share of dolomite and an ~3.4% share of mullite are characteristic of this area (Fig. 3C).

SEM/EDS STUDY OF MINERAL COMPONENTS

Grains and polymineral, metal-bearing aggregates present in the topsoil vary in size from tenths of a micron to 500 μm (Figs. 4 and 5). Analysis of BSE images from the study areas shows that the frequency and type of metal-bearing phases vary as a function of distance from the former Zn smelter and the type of historical waste material that was deposited in different parts of the city (Table 1).

Zinc-bearing minerals. Zn carbonates, mainly smithsonite ($ZnCO_3$), are the most common Zn-bearing minerals. Monheimite $(Zn,Fe)CO_3$ was also relatively common, as indicated by the presence of Fe in the EDS spectra (Fig. 4A). The Zn carbonate grains are up to 50 μm in size (Fig. 4I, M). They form elongated crystals with a rhombohedral habit, their edges often split and rounded. Smithsonite occurs in association with Zn silicates (Fig. 4A), Pb phosphates (Fig. 4I) and Pb carbonates (Fig. 4M). Submicroscopic grains of Zn carbonates are embedded in aggregates of Fe-Mn oxides and Pb carbonates (Fig. 5F). Zinc silicate hemimorphite is a major metalliferous phase at the former smelter site (Table 1: Area 1). It is represented by crystalline aggregates up to 100 μm in size (Fig. 4B) that build thin tabular crystals in sheaf-shaped or fan-shaped clusters (Fig. 4C, D). Another Zn silicate present in the samples is willemite (Zn_2SiO_4), identified by XRD (Fig. 3B). Zinc sulphides, sphalerite (αZnS) and wurtzite (βZnS), are also present in the topsoil (Table 1). Their isolated grains of up to 100 μm in size are highly weathered (Fig. 4E, F). Zinc was identified in aggregates of Fe (Fig. 4K, M) and Fe-Mn oxides (Fig. 5B, C). This element was also identified in Ca-Al silicates and Ca-Zn aluminosilicate (Table 1).

Lead-bearing minerals. Pb carbonate, cerussite ($PbCO_3$), is most commonly found in the topsoil (Fig. 4A, F, J, K, M). It

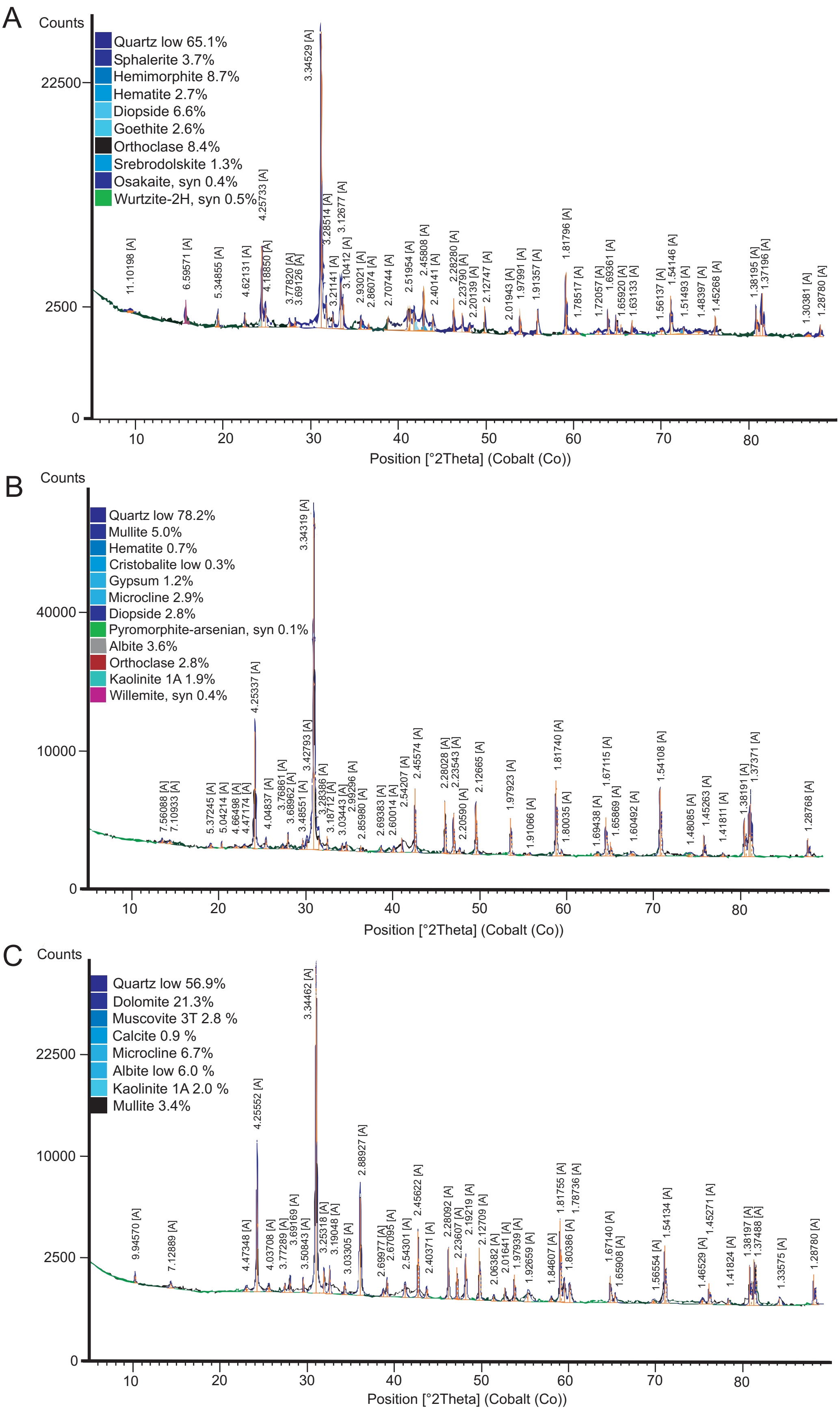

Fig. 3. XRD spectra

A – topsoil sample (SZ14) from Area 1; **B** – topsoil sample (SZ7) from Area 3; **C** – topsoil sample (SZ29) from Area 2; semi-quantitative evaluation of the percentage of minerals

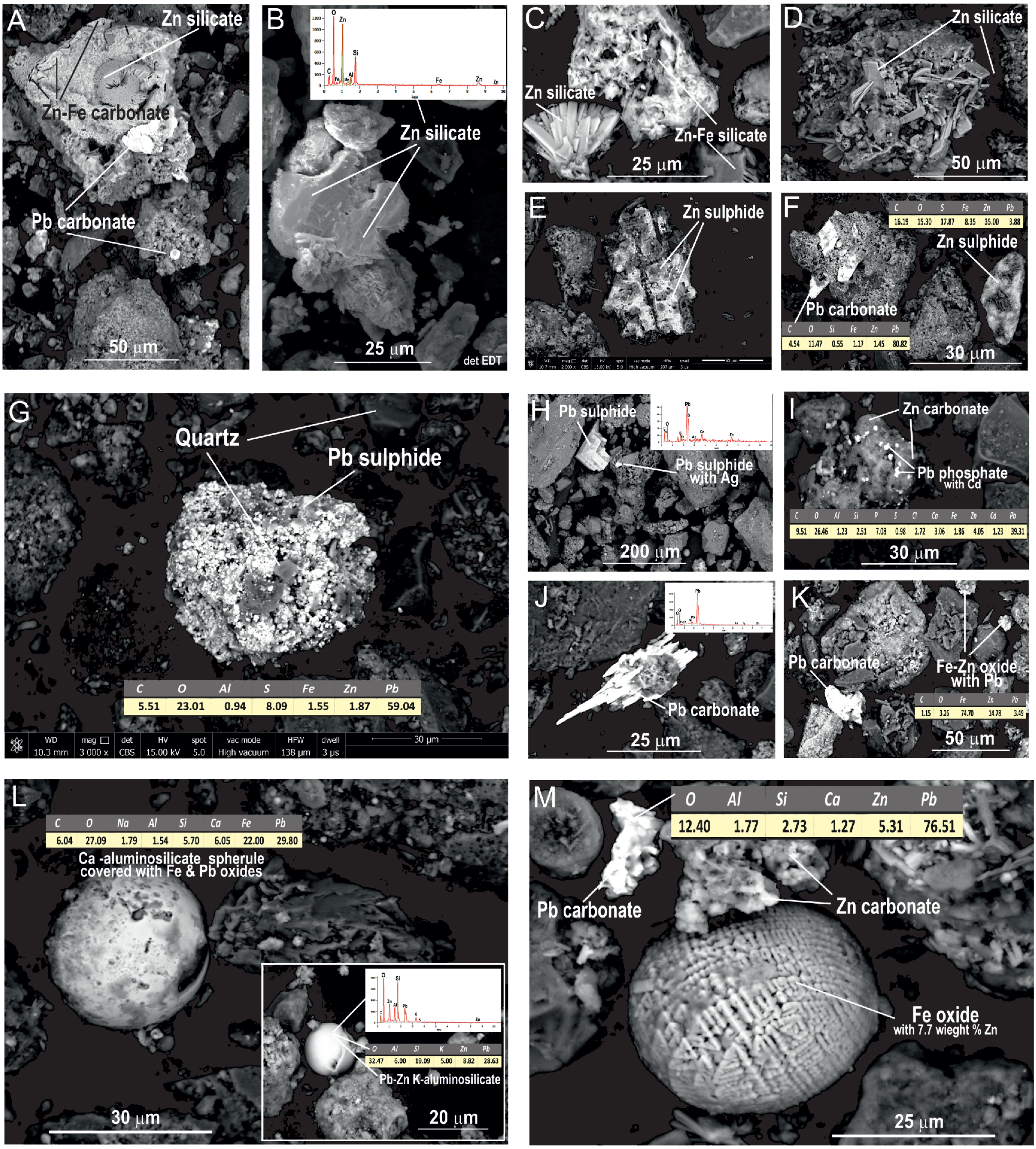

Fig. 4. BSE images of metalliferous minerals from the topsoil in Katowice-Szopienice

builds isolated crystalline grains up to 50 µm in size and occasionally forms aggregates with Fe oxides or Zn silicates. The surfaces of cerussite grains show signs of leaching and weathering.

Galena (PbS), occurs in crystalline, isolated grains (Fig. 4H) or spherical aggregates up to 80 µm in size composed of finely crystalline galena (Fig. 4G). Silver was recognized in a few grains (Fig. 4H), and Ag concentrations were estimated (SEM/EDS) to be 240 mg kg^{-1}. Lead is common in aggregates composed of aluminosilicates, sulphides, carbonates, Zn oxides (Fig. 4F, K) and Fe (Fig. 5C) and Fe-Mn oxides (Fig. 5F). It is derived from submicroscopic grains of Pb oxides and carbonates. The proportion of Pb in these aggregates varies from 3 to 8%. This form of Pb dominates in the topsoil.

Less commonly, Pb phosphates, such as pyromorphite [$Pb_5(PO_4)_3Cl$], were identified. Pyromorphite crystallized on Zn

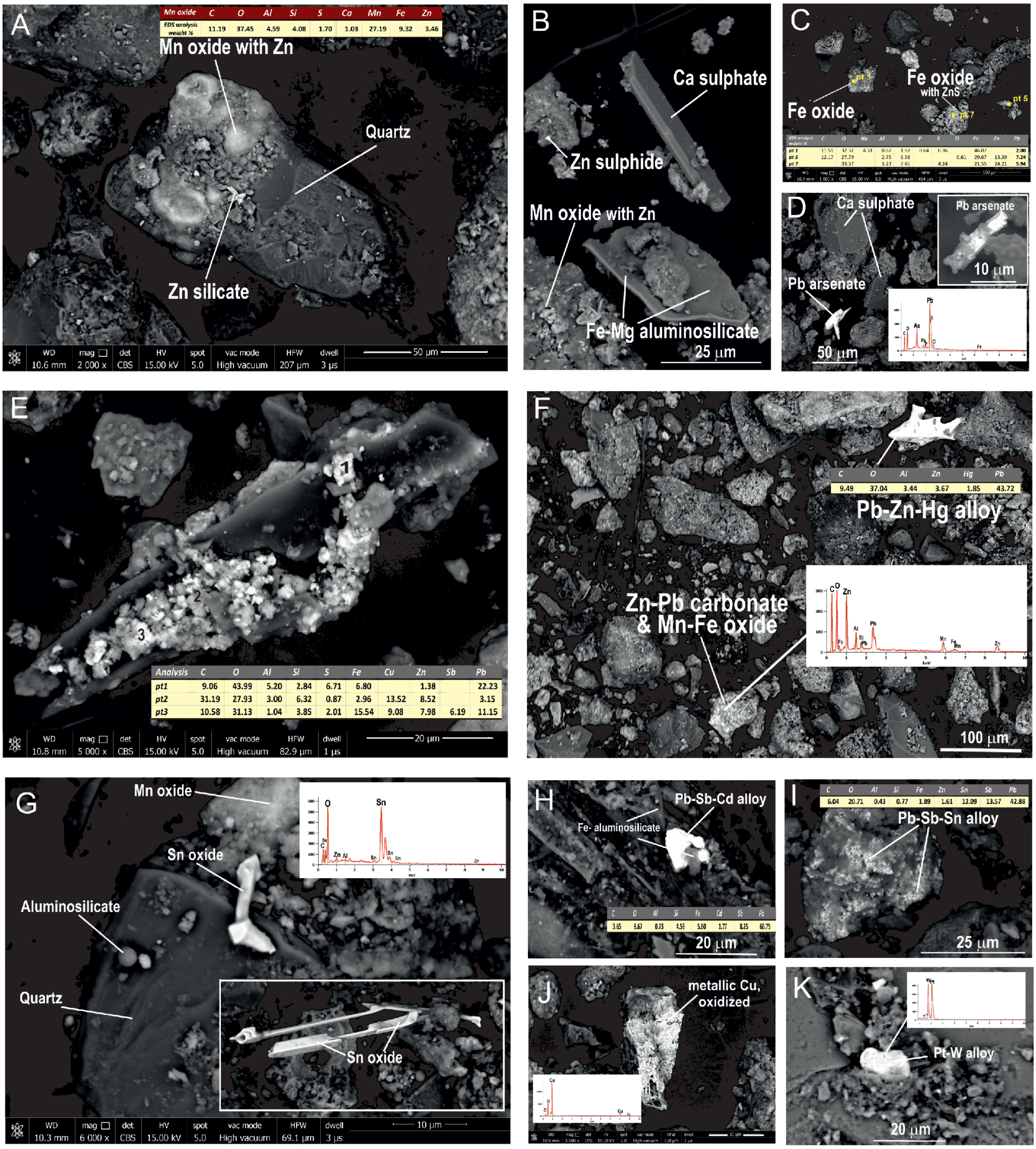

Mn oxide	C	O	Al	Si	S	Ca	Mn	Fe	Zn
EDS analysis weight %	11.19	37.45	4.59	4.08	1.70	1.03	27.19	9.32	3.46

EDS analysis weight %	C	O	Na	Al	Si	P	S	Ti	Fe	Zn	Pb
pt 1	11.51	32.32	4.31	0.87	1.92	0.64	0.36		46.07		2.00
pt 5	12.17	27.79		2.75	6.38			0.61	29.67	13.39	7.24
pt 7		33.37		3.23	7.46		4.24		21.55	24.21	5.94

Analysis	C	O	Al	Si	S	Fe	Cu	Zn	Sb	Pb
pt1	9.06	43.99	5.20	2.84	6.71	6.80		1.38		22.23
pt2	31.19	27.93	3.00	6.32	0.87	2.96	13.52	8.52		3.15
pt3	10.58	31.13	1.04	3.85	2.01	15.54	9.08	7.98	6.19	11.15

C	O	Al	Zn	Hg	Pb
9.49	37.04	3.44	3.67	1.85	43.72

C	O	Al	Si	Fe	Cd	Sb	Pb
3.65	8.67	0.73	4.59	5.60	1.77	8.25	66.75

C	O	Al	Si	Fe	Zn	Sn	Sb	Pb
6.04	20.71	0.43	0.77	1.89	1.61	12.09	13.57	42.88

Fig. 5. BSE images of metalliferous minerals from the topsoil in Katowice-Szopienice

carbonates (Fig. 4I), forming isolated grains of submicroscopic size (<1 µm) which resulted from initial crystallization in the weathering stage. Pb arsenates were also present (Fig. 5D). Lead phases (29.8%) also include synthetic phases represented by:

– spheroidal (up to 30 mm), polymineralic phases in the form of spherules composed of aluminosilicates and oxides of Fe and Pb, and Pb and Zn (Fig. 4L),

– metallic Pb and its alloys with other metals, e.g., Pb-Zn-Hg (Fig. 4F), Pb-Sb-Cd (Fig. 5H), Pb-Sb-Sn (Fig. 5I). Pb-alloy grains range 10 to 100 µm in size.

Minerals with Fe. The main phases with which Fe is associated are oxides (goethite and hematite), Fe-Mn oxides and Fe-Zn oxides (Figs. 4K, M and 5A, C). Less commonly, Zn-Fe carbonates were identified (Fig. 4A). Iron occurs in polymetallic phases of varying composition (Fig. 5F). Iron sulphide grains were identified relatively rarely. Iron is also present in Fe and Fe-Mg aluminosilicates (Fig. 5B, H) and phases formed by high-temperature combustion processes, e.g., aluminosilicate spherulites (Fig. 4L) and srebrodolskite.

Cadmium-bearing minerals. Minerals in which Cd could be identified were rarely found in the soils studied. Cadmium concentrations identified by SEM/EDS in Zn sulphides ranged from 100 to 300 mg kg^{-1}. Much higher concentrations of Cd (up to 12,300 mg kg^{-1}) were identified in Cd-bearing Pb phosphates that were difficult to identify (Fig. 4I).

Minerals with Cu. Copper content (9 to 13.5%) was found in fine-crystalline aggregates with Pb, Zn, Sb and Fe (Fig. 5E). Isolated (80 µm) grains of metallic copper (Fig. 5J) or its alloys with Sn were also found.

Minerals with As and Sb. The As-bearing mineral in the topsoil is mimetite [$Pb_5(AsO_4)_3Cl$] occurring in isolated crystalline grains up to 50 µm in size (Fig. 5D). It occurs in association with Ca sulphates (gypsum), which may indicate its secondary genesis. Antimony was identified in Pb-Sb-Cd alloys (Fig. 5H) and Pb-Sb-Sn alloys (Fig. 5I). In the areas of the former Rolling Mill (Area 2), Pb alloys with Sn in the topsoil are present; cassiterite (Fig. 5G) is also common.

Sulphates and carbonates. Barite ($BaSO_4$) in the form of automorphic, locally over-melted crystals is commonly present in the soils studied, as it is a primary mineral associated with Zn-Pb ores (Cabala et al., 2008, 2020). Submicroscopic gypsum crystals ($CaSO_4 \cdot 2H_2O$) formed by sulphide oxidation processes abound in some topsoils (Figs. 3B and 5B).

HEAVY METAL AND METALLOID CONCENTRATIONS

The concentrations of heavy metals, metalloids and S in the topsoil of the former smelter and adjacent areas vary considerably among the study areas (Table 2 and Fig. 6).

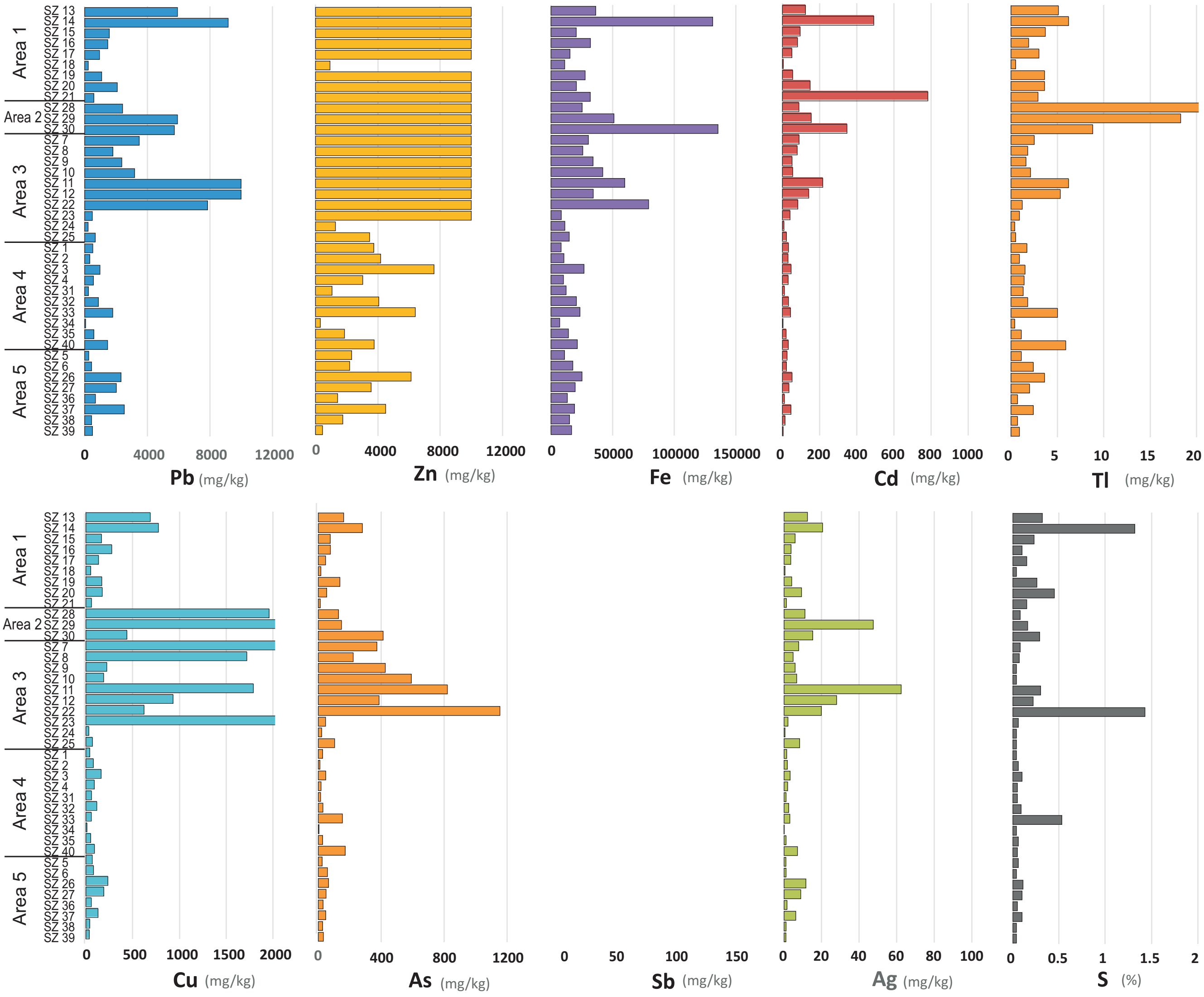

Fig. 6. Concentrations of selected elements in topsoils from the Katowice-Szopienice industrial area

The 10,000 mg kg^{-1} values indicated for Zn and Pb are the upper detection limit values for the MA 250 procedure

Area 1. All the topsoil samples contain >10,000 mg kg^{-1} Zn. Lead concentrations vary from 230 to 9,177 mg kg^{-1}. Iron content ranges from 1.1 to 13.1%. Cadmium concentrations are high, ranging from 51 to 783 mg kg^{-1}. Concentrations of Cu (up to 2,248 mg kg^{-1}), As (up to 280 mg kg^{-1}), Sb (up to 45 mg kg^{-1}) and S (up to 1.43%) are high in some samples.

Area 2. Lead content ranges from 2,424 to 5,927 mg kg^{-1}. Zn content is higher than 10,000 mg kg^{-1}. There are very high concentrations of Fe (up to 13.5%) Cd (up to 347 mg kg^{-1}), Tl (up to 20.5 mg kg^{-1}), As (up to 412.1 mg kg^{-1}), Sb (up to 109.0 mg kg^{-1}), Cu (up to 2,248.5 mg kg^{-1}) and Sn (up to 105.4 mg kg^{-1}) (Table 2).

Area 3. Lead concentrations vary from 211 to over 10,000 mg kg^{-1}. The zinc content of most samples exceeds 10,000 mg kg^{-1}. Cadmium concentrations vary from 8 to 217 mg kg^{-1}. Contents of Cu (up to over 10,000 mg kg^{-1}), Sn (up to 307 mg kg^{-1}), As (up to 1,153 mg kg^{-1}) and Sb (up to 145 mg kg^{-1}) are very high. Sulphur concentrations are also elevated (up to 1.43%).

Area 4. Lead content ranged from 59 to 1,793 mg kg^{-1}. Zinc content ranged from 1,054 to 7,601 mg kg^{-1}. Cadmium concentrations of up to 47 mg kg^{-1} and elevated As content (153 and 171 mg kg^{-1}) were found in two samples (Table 2). For Fe, Cu, Sb, Sn, Ba and S, no concentrations significantly different from typical soils in southern Poland were identified.

Area 5. Lead concentrations ranged from 252 to 2,533 mg kg^{-1}. Zinc concentrations were up to 6,129 mg kg^{-1}, and Cd concentrations were up to 52 mg kg^{-1} (Table 2).

TOPSOIL METAL LEACHING

Zinc. The highest Zn content (278 mg kg^{-1}) in the ion-exchange fraction (F1) was found in sample SZ14, taken from the former smelter site (Area 1). The percentage of Zn in the ion exchange fraction (F1) in the topsoil samples ranged from 0.4 to 2.8%. The highest level of 2.8% was found in sample SZ33 from Area 2. The majority of Zn (30–70%) is bound in the carbonate fraction (F2) (Fig. 7). Between 20 and 25% of Zn is bound to Fe-Mn oxides (F3). The proportion of Zn bound in the organic fraction (F4) is usually <3%. In the residual fraction (F5), 8% to >50% of Zn is bound (Fig. 7).

Lead. Between 0.5 and 0.6% Pb is accumulated in the ion exchange fraction (F1). Only in sample SZ22 (Area 3) is the proportion high (2.3%; Fig. 7). Most Pb (from 34 to 75%) is bound in the carbonate fraction (F2). Between 15 and 45% of Pb are accumulated in Fe-Mn oxides (F3). Between 1 and 7.5% of Pb are bound to the organic fraction (F4); in sample SZ14 (Area 1), as much as 11.1% of Pb is bound to the F4 fraction (Fig. 7). Between 3 and 23 % of Pb accumulates in the residual fraction.

Cadmium. A significant proportion of Cd is in the ion-exchange fraction (F1) (17 to 23% of the total Cd pool; Fig. 7). Between 28 and 58% of Cd are associated with the carbonate fraction, and between 10 and 22% of Cd are associated with Fe-Mn oxides. The organic fraction (F4) contains 1.4 to 7% Cd. The remaining Cd accumulates in the residual fraction.

Copper. This accumulates mainly in the carbonate fraction and Fe-Mn oxides. The proportion of Cu in the organic fraction (F4) is surprisingly high, between 16 and 66% (Fig. 7). The remaining Cu is bound to the insoluble residual fraction. The highest total Cu content was found in sample SZ7 (10,000 mg kg^{-1}) and the lowest (57 mg kg^{-1}) in sample SZ33.

DISCUSSION

Zinc, Pb and Cd contamination of soils around Zn-Pb smelters is most often associated with atmospheric deposition of metal-bearing mineral particles (Deng et al., 2016). However, after smelter closure, the greatest environmental risk is associated with post-smelter waste and topsoil enriched in metal-bearing minerals left on the surface (Kierczak et al., 2010; Stafilov et al., 2010; Tyszka et al., 2014; Kicińska, 2020; Cabała et al., 2020; Pasieczna et al., 2020; Guillevic et al., 2023). The topsoil around the historic smelters in Szopienice contains significant amounts of Zn and Cd bound in sulphides (sphalerite and wurtzite), silicates (hemimorphite, willemite), carbonates (cerussite, smithsonite), Fe and Fe-Mn oxides and synthetic silicates. Zn sulphates are also present, such as osakaite identified in the topsoil. This mineral is a product of secondary transformations of Zn sulphides (Ohnishi et al., 2007). Its presence indicates that oxidation processes of relict Zn sulphide are active.

Dominant among the Zn-bearing minerals are:

sphalerite and wurtzite > smithsonite > hemimorphite > willemite > Zn oxide > Fe-Zn oxide > aluminosilicate aggregates with Zn > Zn sulphates (e.g., osakaite)

SEM-EDS studies clearly show that, in samples from Areas 1–3, sulphides, carbonates, zinc silicates and Zn-rich Fe-Mn oxides and aluminosilicates are very common. In addition, XRD studies confirmed the high proportion of sphalerite, wurtzite and hemimorphite in the topsoil from Area 1. The significant proportion of Zn-rich, Pb-rich, Fe-rich minerals results in high concentration levels of these metals. Similarly high concentrations have been identified for geochemically sulphide-bound elements such as Cd, As, Sb and Tl. Approximately 40% of the charge for Zn production in the Szopienice smelters were concentrates from supergene-type deposits occurring in the Bytom and Olkusz areas. Hemimorphite and smithsonite were constituents of non-sulphide, galman-type ores that formed in shallow weathering zones (Cabala, 2001; Coppola et al., 2009). Willemite was also identified in the topsoil near the former smelter (Table 1). This mineral does not occur in the Silesian-Kraków deposits. It may form by weathering processes of smelter slags and has been found in smelter dumps in Świętochłowice (southern Poland) (Bril et al., 2008). Willemite can be formed as a result of weathering changes in hemimorphite; the reverse reaction is also possible (Vanaecker et al., 2014). Willemite grains present in the topsoil may be an indicator of contamination by weathering smelter slags. Zinc-enriched silicate phases, products of high-temperature metallurgical processes (e.g., diopside, mullite, cristobalite), were also identified in the topsoil (Fig. 3). Zinc is often present in synthetic silicates and oxides (Warchulski et al., 2015; Sobanska et al., 2016). The Zn sulphides dispersed in the soil originated from sphalerite concentrates, which were the raw material for Zn production. However, they were rarely identified, suggesting that the submicroscopic ZnS grains had been oxidized.

Among the Pb-containing minerals in the topsoil, cerussite clearly dominates. The relative abundance of lead-bearing minerals (based on SEM-EDS studies) is:

cerussite > galena > Fe-Mn oxide with Pb > pyromorphite > mimetite > aluminosilicates with Pb > Pb-rich alloys

Cerussite and galena come from Zn-Pb ores of galman-type, which were long the main raw material for Zn production in

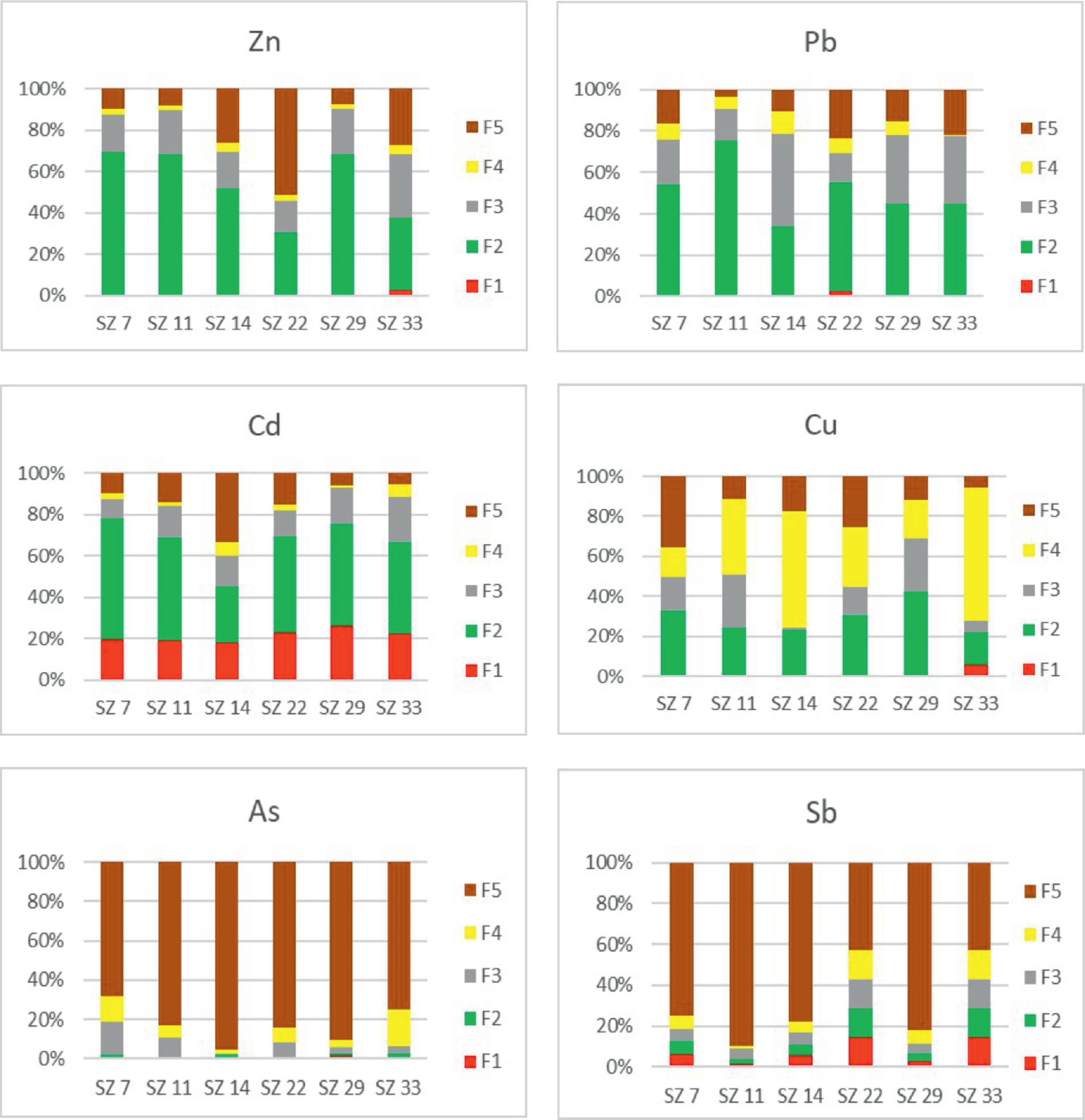

Fig. 7. Leachability of Zn, Pb, Cd, Cu, As and Sb from topsoil samples in Katowice-Szopienice, using the Tessier et al. (1979) method

F1 – ion-exchange fraction, F2 – carbonate fraction, F3 – fraction associated with Fe and Mn oxides, F4 – organic fraction, F5 – residual fraction (Appendix 2)

Szopienice. These ores contained relict galena, the proportion of sulphide-bound Pb sometimes approaching several percent (Cabala, 2001; Coppola et al., 2009). Therefore, galena was identified in topsoil from Areas 1 and 3, where ore was stored and prepared for the smelting process. In other areas, galena was not identified.

The submicroscopic Pb-rich phases emitted by smelters are most commonly PbS, $PbSO_4$ and $PbSO_4$ × PbO (Sobanska et al., 1999; Soto-Jiménez et al., 2023), which are unstable in the soil environment. Manganese and Fe oxides, especially synthetic phases, have a high capacity to be retained and stabilize Pb^{2+} ions (O'Reilly and Hochella, 2003). Therefore, Pb was often identified in aggregates of Fe, Fe-Mn, Zn oxides (Fig. 4K, C) and aluminosilicates.

The rare occurrence of Pb phosphates, probably pyromorphite, is restricted to submicroscopic phases (Fig. 4I). Pyromorphite probably formed secondarily in an environment enriched in Pb^{2+} and phosphate ions (Burmann et al., 2013; Cabala et al., 2020). Flis et al. (2011) indicated a strong tendency for pyromorphite to partition into a solid phase in the pyromorphite-mimetite series. An improvement in the stability of the mimetite lattice was observed due to isostructural phosphate substitutions at anionic sites. In the topsoil from Szopienice, mimetite was more frequently identified from the promorphite-mimetite series. It is likely that the pool of arsenic ions in the weathering products of Zn-Pb ore minerals is larger than that of phosphate ions. In the weathering products of slags from Zn metallurgy, pyromorphite is reported relatively rarely (Nadłonek et al., 2024).

In the topsoil investigated, mimetite was identified as submicroscopic grains (Fig. 5C, D). Mimetite has been reported in smelter slags in various areas of the Silesian-Kraków region (Bril et al., 2008; Nadłonek et al., 2024). Submicroscopic aggregates of mimetite were recognized in association with gypsum, indicating its secondary genesis. Lead also occurs in the structure of silicates formed in metallurgical processes (Sobanska et al., 2016). Fine grains of alloys of Pb with other metals (Sb, Sn, W, Zn, Hg) (Fig. 5F, H, I, K) emitted by metallurgical plants operating in Szopienice in the second half of the 20th century were also a Pb source. Metallic Pb and Pb-antimony alloys were only identified in the area of the former Rolling Mill and Bernhardi smelter (Table 1: Area 2). Pb-Sb alloy grains are indicative of historical Sb-cured Pb production. Pb-Sn alloys have been used as soft binders, for soldering, in the electronics and electrical industry, and in the manufacture of ammunitions. Identifying the composition of the alloys dispersed in the topsoil makes it possible to indicate the type of historical production.

The concentration of Cd at the former smelter (Area 1) and in adjacent areas often exceeds 50 mg kg^{-1}. The extremely high Cd concentration of 783 mg kg^{-1} (Table 2) is comparable to the Cd content (1,033 to 5,741 mg kg^{-1}) found in sphalerites from the Silesian-Kraków deposits (Mikulski et al., 2020).

The highest Cd content was recorded in topsoil rich in Zn and S (Table 2), corroborating that Cd is mainly associated with Zn sulphides or carbonates (Viets et al., 1996; Mikulski et al., 2020). A slight enrichment in Cd at the grain margins of Pb phosphate aggregates (Fig. 4I) and Pb-Sb alloys (Fig. 5H) was observed. This indicates a high potential for the mobilization of Cd from slags into the environment (cf. Tyszka et al., 2018).

The few submicroscopic spherules observed in Szopienice topsoil contain Pb (Fig. 4L); they are more often composed of aluminosilicates (Fig. 5G). In areas adjacent to Zn smelters, metal-bearing spherical phases are commonly represented in topsoil (Cabała and Teper, 2007). Their spherical forms indicate that they are the result of emissions from high-temperature metallurgical processes or fossil fuel combustion (Rożek et al., 2015; Soto-Jiménez et al., 2023). Except for a few, no Zn- or Pb-rich spherical aggregates were identified in the topsoil of Szopienice affected by historical Zn and Pb smelting. It is likely that the submicroscopic spherical phases undergo chemical transformations in the topsoil and are dissolved, and therefore historical emissions from Zn smelters cannot be documented.

The significant size (several tens to hundreds of microns) and the forms of metal-bearing constituents indicate that the topsoil at Szopienice was enriched in fractions originating from former stockpiles of raw materials fed into the metallurgical process and from post-smelting waste (slag). The mineral composition of the slag-derived fractions is similar to that of waste from other smelters in the Silesian-Kraków region (Tyszka et al., 2014; Warchulski et al., 2015).

ENVIRONMENTAL RISKS OF METAL LEACHING

In soils contaminated with metallurgical waste, the leachability of Zn, Pb and Cd is controlled by the reactivity and weathering transformations of high-temperature mineral phases (Cappuyns et al., 2014). Metals (Zn, Pb, Cd, Tl) present in the primary phases (Zn-Pb sulphides, Zn and Pb carbonates) under conditions of lowered pH of the soil environment are more easily leached into the environment.

The release of heavy metal cations to the water phase ("leaching potential"), and their mobility, depend on their solution speciation, and their affinity to bind to reactive surfaces in the soil matrix and pore water [such as particulate and dissolved organic matter, clays or metal (hydr)oxide-surfaces] (Dijkstra et al., 2004). This process is influenced by several factors, including soil pH, the presence of organic matter, and the specific chemical properties of the heavy metals themselves. Acidic conditions generally promote leaching, while alkaline conditions can lead to greater retention.

The leaching potential of Zn from the topsoil studied is low, as the metal is mainly bound in carbonate (30 to 70%) or the residual fraction (10 to 50%). Under low moisture, Zn carbonates and silicates are relatively stable, and leaching of Zn^{2+} ions is limited. However, under waterlogged conditions, Zn carbonates may dissolve over longer periods of time and provide a source of Zn^{2+} ions (Van Damme et al., 2010; Jerzykowska et al., 2014). Mineral release analyses (MLA) by Xu et al. (2022) showed that As, Cd, Pb and Zn bound in silicate phases were stable and weakly leached over long periods of time and under the low pH of the soil environment.

Also present in the residual fraction are slag-derived minerals in which Zn is incorporated into the silicate structure of high-temperature phases, such as spinel, melilite and pyroxene (Warchulski et al., 2015). Zinc also occurs in aggregates of Fe, Mn oxides (Figs. 4M and 5A,C) and sheet aluminosilicates. These types of Zn-bearing minerals favour the stabilization and immobilization of Zn in the soil environment; however, Zn^{2+} mobility may increase under long-term weathering and, for example, low pH conditions (Jerzykowska et al., 2014). Nachtegaal et al. (2005) indicated that there is a risk of increased leaching of Zn from fractions considered stable (e.g., carbonate or oxide) under conditions of a significant decrease in environmental pH over a long period of time.

The leachability of Pb from the topsoils investigated (Fig. 6) is low, the highest amount of this metal being bound in the carbonate fraction and in Fe-Mn oxides. Lead in the residual fraction probably came from metallurgical products (slags), as indicated by Guillevic et al. (2023). The presence of small aggregates with Pb phosphates (Fig. 4I) indicates that Pb^{2+} ion activation processes proceed only on the microscopic scale. The weathering transformation of Pb-rich mineral phases leads to the formation of cracks and fills with secondary Pb minerals such as the Pb sulphates $3PbO \times PbSO_4$ and $4PbO \times PbSO_4$ (Sobanska et al., 2016). The formation of Pb sulphates increases the potential for Pb leaching into the environment.

Cadmium has the highest leaching potential. More than 20% of this metal is present in the ion exchange fraction (Fig. 6) while 30 to 50% occur in the carbonate fraction. With high total Cd content in Areas 1–3 (exceeding 50 mg kg^{-1}), the risk of transfer of high Cd loads from the topsoil to the environment is serious. In soils of the Silesian-Kraków region, Kicińska (2019) estimated the proportion of the ion-exchangeable fraction of Cd to be 20%, indicating a very high risk ($50 \leq$ RAC, risk assessment code). Carbonate minerals are acid-sensitive; lowering the pH in the soil can increase leaching of Cd and Pb (Liu et al., 2018). Our study shows that waste and emissions from ore smelting are dangerous due to the release of Cd ions. This is because Cd concentrations are high in Zn sulphides from Silesian-Kraków deposits. Cadmium concentrations are commonly higher than the permissible content of 15 mg kg^{-1} (Polish

Regulation, 2016 – Polska Norma). In addition, if the pH of the soil environment is permanently lowered, the pool of bioavailable Cd and Zn could increase significantly (Cappuyns et al., 2014). Very high, often extreme, metal contents in top-soil from Szopienice have also been indicated when studying soil flora and microorganisms (Gzyl, 1997; Badora et al., 1998; Kuźniar et al., 2018). Extremely high contents of PHEs were also noted in the region studied by the Polish Geological Survey (Konon et al., 2024) for Zn (2,500 mg kg^{-1} to max. 36,510 mg kg^{-1}), Cd (32–128 mg kg^{-1}), Pb (500–5,000 mg kg^{-1}) and As (40–320 mg kg^{-1}).

Copper is bound to the carbonate, organic and residual fractions (Fig. 6), and only under conditions of reduced pH of the soil environment can it be leached into the environment. This applies also to other metals that are bound only in carbonates, oxides or silicates.

The metalloids As and Sb accumulate mainly in the residual fraction, indicating their limited leaching potential. A few to 15% of Sb is present in the ion-exchange fraction, so some may be leached into the environment.

The total concentrations of Zn, Pb and Cd in topsoil in these historical metallurgical areas strongly exceed acceptable standards and commonly range from 2,000 to 2,300 mg kg^{-1} for Pb, 3,500 to 6,000 mg kg^{-1} for Zn and 30 to 52 mg kg^{-1} for Cd (Appendix 1). The very high concentrations of toxic Pb, As and Cd in the former smelting areas (Table 2) are confirmed by the high ratios of As/Pb, Sb/Pb and Cd/Pb normalized to Pb = 1,000 mg kg^{-1}. The ratios for As and Sb (Table 2) are similar to those reported at Pb smelters in the USA (Kimbrough and Cardner, 1999; Eckel et al., 2002). Significantly higher values were calculated for Cd/Pb (Table 2), which indicates that the historical Zn and Pb smelting in Szopienice released significant Cd amounts into the soils. Large-scale production of Cd metal or Cd sponge was possible because the Silesian-Kraków Zn-Pb ores are characterized by high concentrations of this element (Viets et al., 1996; Cabala, 2001; Tyszka et al., 2018; Gorecki, 2018; Mikulski et al., 2020).

The most important causes of the enrichment of the topsoil studied in metal-rich minerals, as a consequence of heavy Zn, Pb and Cd contamination, include:

– the long duration (180 years) of continuous production of Zn, Pb and alloys with non-ferrous metals and related emission of metal-bearing dusts into the atmosphere,

– the large-scale production of Zn, Pb and Cd in several smelters located in Szopienice (Fig. 1);

– the largest Zn smelter occupied an area of ~63 hectares, where batch raw materials and post-production waste were stored;

– in the areas adjacent to the smelter, purchased by the owners of the smelters, waste from metallurgical processes was deposited in an unsystematic manner.

This is indicated by the presence of grains probably representing high-temperature, synthetic phases (e.g., mullite, aluminosilicate spherules with Pb, diopside) that may have been formed in the Zn smelting process.

SUMMARY AND CONCLUSIONS

180 years of Zn and Pb metallurgy have resulted in extremely high concentrations of Zn, Pb, Cd and As in the topsoil around Szopienice as a result of atmospheric emissions, resuspension and deposition of metal-bearing waste. The sites of former smelters and their surroundings are the most polluted; however, dispersion of metals from Zn and Pb smelting occurred throughout the Szopienice district. Large-scale metallurgical production of Zn and Pb and the metallurgy of Pb-Sb and Cu alloys resulted in large areas occupied by various types of raw material dumps (oxidized ores, sulphide concentrates, processed Pb-Sb alloys) and tailings. Minerals from metallurgical waste or historical emissions are found in areas around the Rawa River, playgrounds, parks and city squares. During the 19th and 20th centuries, waste material from smelters was probably used for road foundations and railroad embankments and in landfills. The surface of the soils has been sealed with asphalt roads and industrial buildings, or covered by cobblestones. As a result of reclamation work, most metallurgical waste and contaminated soils have been buried below the surface. At present, they pose only a potential threat to the environment. However, in cases of land redevelopment and accompanying changes in the flow of shallow circulating waters, buried, metal-rich waste may again threaten the environment.

Our study of metal-bearing soil minerals can facilitate the development of more effective remediation strategies for post-smelter sites and deepen the scientific understanding of the dynamics of the release of major contaminants into the environment. Metal-rich topsoil overlying post-smelter landfills requires remediation work, as erosion, aeolian transport and surface runoff processes can spread fine metal-bearing fractions to more distant areas.

CONCLUSIONS

1. The metalliferous minerals identified in the topsoil most likely come from long-term emissions, the source of which was the landfills. These were a determining factor in the high concentrations of Zn, Pb, Cd and As in the topsoil.

2. The very common occurrence of Zn silicate and Zn carbonate grains in the area of the former Uthemann Zn smelter shows that Zn production was based, to a large extent, on oxidized ores (galman-type).

3. In former smelting areas and their neighbourhood in Szopienice the most frequently identified metalliferous minerals were smithsonite, hemimorphite and cerussite. Part of the Zn, Pb, Cd is bound in Fe-Mn oxides and aluminosilicates.

4. Zinc and Cd were also identified in Fe, Fe-Mn oxide aggregates and aluminosilicates. This may be the result of secondary processes and sorption of these metals by iron oxides and aluminosilicates.

5. Metallic Pb and its alloys, such as Pb-Sb and Pb-Sb-Sn, were identified in the topsoil at the former Rolling Mill and in the vicinity of the Walter Croneck smelter. We have shown that SEM/EDS studies can identify the type of production that was the source of contamination (for example, whether metals or metalloids were used).

6. Pb concentrations in the topsoil are frequently higher than 600 mg kg^{-1}, exceeding the limit value for industrial sites (Polish Regulation, 2016 – Polska Norma). The high total Pb content comes mainly from Pb carbonates and Pb alloys. These phases are stable under weathering conditions, so the environmental risk of Pb^{2+} ion mobilization is relatively low.

7. Zinc concentrations commonly exceed several thousand mg kg^{-1}. Zinc mineral phases, represented mainly by carbonates, oxides and silicates, are stable in the soil and are therefore not a source of Zn^{2+} ions for the environment.

8. The Cd content in the samples frequently exceeds 50 mg kg^{-1}. The results of leachability studies, especially the high Cd content in the ion exchange fraction, indicate that there is a significant risk of transfer of this toxic element to the environment.

Acknowledgements. The research was co-financed by the 'Green Horizon' project (2021–2023) carried out at the University of Silesia in Katowice.

REFERENCES

Anyadike, N., 2002. Lead and Zinc: Threats and Opportunities in the Years Ahead. Woodhead Publishing Limited, Abington Cambridge.

Badora, A., Furrer, G., Grünwald, A., Schulin, R., 1998. Immobilization of zinc and cadmium in polluted soils by polynuclear Al13 and Al-montmorillonite. Journal of Soil Contamination, **7**: 573–588; https://doi.org/10.1080/10588339891334447

Burmann, F., Keim, M.F., Oelmann, Y., Teiber, H., Marks, M.A.W., Markl, G., 2013. The source of phosphate in the oxidation zone of ore deposits: evidence from oxygen isotope compositions of pyromorphite. Geochimica et Cosmochimica Acta, **123**: 427–439; https://doi.org/10.1016/j.gca.2013.07.042

Bril, H., Zainoun, K., Puziewicz, J., Courtin-Nomade, A., Vanaecker, M., Bollinger, J-C., 2008. Secondary phases from the alteration of a pile of zinc-smelting as indicators of environmental conditions: an example from Świętochłowice, Upper Silesia, Poland. The Canadian Mineralogist, **46**: 1235–1248; https://doi.org/10.3749/canmin.46.5.1235

Cabala, J., 2001. Development of oxidation in Zn-Pb deposits in Olkusz area. In: Mineral Deposits at the Beginning of the 21st century (ed. A. Piestrzyński): 121–124, Balkema; https://doi.org/10.1201/9781003077503

Cabala, J., Teper, L., 2007. Metalliferous constituents of rhizosphere soils contaminated by Zn-Pb mining in southern Poland. Water, Air and Soil Pollution, **178**: 351–362; https://doi.org/10.1007/s11270-006-9203-1

Cabala, J., Zogala, B., Dubiel, R., 2008. Geochemical and geophysical study of historical Zn-Pb ore processing waste dump areas (Southern Poland). Polish Journal of Environmental Studies, **17**: 693–700.

Cabała, J., Warchulski, R., Rozmus, D., Środek, D., Szełęg, E., 2020. Pb-rich slags, minerals, and pollution resulted from a medieval Ag-Pb smelting and mining operation in the Silesian-Cracovian Region (Southern Poland). Minerals, **10**, 28; https://doi.org/10.3390/min10010028

Cabała, J., Janeczek, J., Kowalczyk, A., 2021. Lead in the environment. Nr specjalny "Narracje o Zagładzie": Ołów/ołowica w kulturze i nauce: 147–223, Wydaw. Uniwersytet Śląski; https://doi.org/10.31261/NoZ.2021.DHC.09

Cappuyns, V., Alian, V., Vassilieva, E., Swennen, R., 2014. pH dependent leaching behaviour of Zn, Cd, Pb, Cu and As from mining wastes and slags: kinetics and mineralogical control. Waste and Biomass Valorization, **5**: 355–368; https://doi.org/10.1007/s12649-013-9274-3

Charkiewicz, A.E., Backstrand, J.R., 2020. Lead Toxicity and Pollution in Poland. International Journal of Environmental Research and Public Health, **17**, 4385. https://doi.org/10.3390/ijerph17124385

Coppola, V., Boni, M., Gilg, H.A., Strzelska-Smakowska, B., 2009. Nonsulfide zinc deposits in the Silesia-Cracow district, Southern Poland. Mineralium Deposita, **44**: 559–580; https://doi.org/10.1007/s00126-008-0220-4

Ćwieląg-Drabek, M., Piekut, A., Gut, K., Grabowski, M., 2020. Risk of cadmium, lead and zinc exposure from consumption of vegetables produced in areas with mining and smelting past. Scientific Reports, **10**, 3363; https://doi.org/10.1038/s41598-020-60386-8

Dalton, C.B., Bates, L.I., 2005. Impact of closure of a large lead-zinc smelter on elevated blood lead levels of children in adjacent suburbs, Boolaroo, Australia. Environmental Exposure and Health. WIT Transactions on Ecology and the Environment, **85**: 377–387.

Deng, W., Li, X., An, Z. Yang, L., 2016. Lead contamination and source characterization in soils around a lead-zinc smelting plant in a near-urban environment in Baoji, China. Archives of Environmental Contamination and Toxicology, **71**: 500–508; https://doi.org/10.1007/s00244-016-0317-1

Dijkstra, J.J., Meeussen, J.C.L., Comans, R.N.J., 2004. Leaching of heavy metals from contaminated soils: an experimental and modeling study. Environmental Science and Technology, **38**: 4390–4395; https://doi.org/10.1021/es049885v

Dungworth, D., White, H., 2021. Scientific examination of zinc-distillation remains from Warmley, Bristol. Historical Metallurgy, **41**: 77–83; https://hmsjournal.org/index.php/home/article/view/223

Eckel, W.P., Rabinowitz, M.B., Foster, G.D., 2002. Investigation of unrecognized former secondary lead smelting sites: confirmation by historical sources and elemental ratios in soil. Environmental Pollution, **117**: 273–279; https://doi.org/10.1016/S0269-7491(01)00195-6

Flis, J., Manecki M., Bajda T., 2011. Solubility of pyromorphite Pb5(PO4)3Cl-mimetite Pb5(AsO4)3Cl solid solution series. Geochimica et Cosmochimica Acta, **7**: 1858–1868; https://doi.org/10.1016/j.gca.2011.01.021

Gorecki, W., 2018. Rozwój przemysłu na Górnym Śląsku w XVIII i XIX wieku (in Polish). Silesia Progress.

Guillevic, F., Rossi, M., Develle, A-L., Spadini, L., Martins, J.M.F., Arnaud, F., Poulenard, J., 2023. Pb dispersion pathways in mountain soils contaminated by ancient mining and smelting activities. Applied Geochemistry, **150**: 105556; https://doi.org/10.1016/j.apgeochem.2022.105556

Gzyl, J., 1997. Assessment of Polish population exposure to lead and cadmium with special emphasis to the Katowice Province on the basis of metal concentrations in environmental compartments. Central European Journal of Public Health, **5**: 93–96.

Hahn, O.H., 1910. Lead and zinc smelting in Upper Silesia. The Engineering and Mining Journal, **89**: 1111–1114.

Hamilton, A., 1914. Lead Poisoning in the Smelting and Refining of Lead. Bulletin of the United States Bureau of Labor Statistics, **141**.

Hartshorne, R., 1934. The Upper Silesian Industrial District. Geographical Review, **24**: 423–438; https://doi.org/10.2307/208914

Jerzykowska, I., Majzlan, J., Michalik, M., Göttlicher, J., Steininger, R., Błachowski, A., Ruebenbauer, K., 2014. Mineralogy and speciation of Zn and As in Fe-oxide-clay aggregates in the mining waste at the MVT Zn-Pb deposits near Olkusz, Poland. Geochemistry, **74**: 393–406; https://doi.org/10.1016/j.chemer.2014.03.003

Jędryka, M., 2020. "Ołowiane dzieci". Zapomniana epidemia (in Polish). Wydaw. Krytyki Politycznej, Warszawa.

Kabata-Pendias, A., Pendias, H., 1999. Biogeochemia pierwiastków śladowych (in Polish). PWN, Warszawa.

Kicińska, A., 2019. Environmental risk related to presence and mobility of As, Cd and Tl in soils in the vicinity of a metallurgical plant – long-term observations. Chemosphere, **236**, 124308; https://doi.org/10.1016/j.chemosphere.2019.07.039

Kicińska, A.J., 2020. Lead and zinc in soils around a zinc-works – presence, mobility and environmental risk. Journal of Ecological Engineering, **21**: 185–198; https://doi.org/10.12911/22998993/119815

Kierczak, J., Bril, H., Neel, C., Puziewicz, J., 2010. Pyrometallurgical slags in Upper and Lower Silesia (Poland): from environmental risks to use of slag-based products – a review. Archives of Environmental Protection, **36**: 11–126.

Kimbrough, D.E., Cardner, N.H., 1999. Off-site forensic determination of waterborne elemental emissions: a case study at a secondary lead smelter. Environmental Pollution, **106**: 293–298; https://doi.org/10.1016/S0269-7491(99)00113-X

Konon, A., Szczypczyk, A., Kostrz-Sikora, P., Fajfer, J., Szyborska-Kaszycka, J., Strzemińska, K., Pasieczna, A., 2024. Detailed Geochemical Map of Upper Silesia 1:25,000, Siemianowice Śląskie map sheet M-34-63-A-a. Polish Geological Institute-National Research Institute, Warsaw.

Krantz Fr., 1911. Die Entwickelung der oberschlesischen Zinkindustrie in technischer, wirtschaftlicher und gesundheitlicher Hinsicht (in German). Kattowitz O.-S. Verlag von Gebrüder Böhm.

Kuźniar, A., Banach, A.M., Stępniewska, Z., Frąc, M., Oszust, K., Gryta, A., Kłos, M., Wolińska, A., 2018. Community-level physiological profiles of microorganisms inhabiting soil contaminated with heavy metals. International Agrophysics, **32**: 101–109.

Leach, D.L. Bradley, D.C., Dwight, C., Huston, D., Pisarevsky, S.A., Taylor, R.D., Gardoll, S.J., 2010. Sediment-hosted lead-zinc deposits in Earth history. Economic Geology, **105**: 593–625; https://doi.org/10.2113/gsecongeo.105.3.593

Li, P., Lin, C., Cheng, H., Duan, X., Lei, K., 2015. Contamination and health risks of soil heavy metals around a lead/zinc smelter in southwestern China. Ecotoxicology and Environmental Safety, **113**: 391–399; https://doi.org/10.1016/j.ecoenv.2014.12.025

Liu, H., Probst, A., Liao, B., 2005. Metal contamination of soils and crops affected by the Chenzhou lead/zinc mine spill (Hunan, China). Science of The Total Environment, **339**: 153–166. https://doi.org/10.1016/j.scitotenv.2004.07.030

Liu, T., Li, F., Jin, Z., Yang, Y., 2018. Acidic leaching of potentially toxic metals cadmium, cobalt, chromium, copper, nickel, lead, and zinc from two Zn smelting slag materials incubated in an acidic soil. Environmental Pollution, **238**: 359–368; https://doi.org/10.1016/j.envpol.2018.03.022

Mikulski, S.Z., Oszczepalski, S., Sadłowska, K., Chmielewski, A, Małek, R., 2020. Trace element distributions in the Zn-Pb (Mississippi valley-type) and Cu-Ag (Kupferschiefer) sediment-hosted deposits in Poland. Minerals; **10**, 75; https://doi.org/10.3390/min10010075

Nachtegaal, M., Marcus, M.A., Sonke, J.E., Vangronsveld, J., Livi, K.J.T., van Der Lelie, D., Sparks, D.L., 2005. Effects of in situ remediation on the speciation and bioavailability of zinc in a smelter contaminated soil. Geochimica et Cosmochimica Acta, **69**: 4649–4664; https://doi.org/10.1016/j.gca.2005.05.019

Nadłonek, W., Cabała, J., Szopa, K., 2024. Potentially harmful elements (As, Sb, Cd, Pb) in soil polluted by historical smelting operation in the Upper Silesian area (Southern Poland). Minerals, **14**, 475; https://doi.org/10.3390/min14050475

Neisser, E.J., 1907. Internationale Übersicht über Gewerbehygiene nach den Berichten der Gewerbe-Inspektionen der Kulturländer. Bibliothek für Soziale Medizin, Hygiene und Medizinalstatistik und die Grenzgebiete von Volkswirtschaft, Medizin und Technik No 1(in German). Verlag Gutenberg, Berlin.

Ohnishi, M., Kusachi, I., Kobayashi, S., 2007. Osakaite, $Zn_4SO_4(OH)6 \cdot 5H_2O$, a new mineral species from the Hirao mine, Osaka, Japan. The Canadian Mineralogist, **45**: 1511–1517; https://doi.org/10.3749/canmin.45.6.1511

O'Reilly, S.E., Hochella Jr., M.F., 2003. Lead sorption efficiencies of natural and synthetic Mn and Fe-oxides. Geochimica et Cosmochimica Acta, **67**: 4471–4487; https://doi.org/10.1016/S0016-7037(03)00413-7

Osman, K., Björkman, L., Lind, B., Nordberg, M., 1992. Biological monitoring of metals in children and pregnant women in Poland. International Journal of Environmental Health Research, **2**: 212–222; https://doi.org/10.1080/09603129209356755

Pasieczna, A., Konon, A., Nadłonek, W., 2020. Sources of anthropogenic contamination of soil in the Upper Silesian Agglomeration (southern Poland). Geological Quarterly, **64**: 988–1003; https://doi.org/10.7306/gq.1564

Péters, A., 2016. La Vieille-Montagne (1806–1873). Innovations et mutations dans l'industrie du zinc. Liège, Les éditions de la province de Liège. Préface de Christophe Bissery.

Polish Regulation (Polska Norma), 2016. Dz.U. poz.1395 on the Assessment of Ground and Soil Contamination (in Polish).

Rahmonov, O., Cabała, J., Krzysztofik, R., 2021. Vegetation and environmental changes on contaminated soil formed on waste from an historic Zn-Pb Ore-washing plant. Biology, **10**, 1242; https://doi.org/10.3390/biology10121242

Raj, K., Das, A.P., 2023. Lead pollution: Impact on environment and human health and approach for a sustainable solution. Environmental Chemistry and Ecotoxicology, **5**: 79–85; https://doi.org/10.1016/j.enceco.2023.02.001

Rossiter, D.G., 2007. Classification of urban and industrial soils in the World Reference Base for soil resources. Journal of Soils and Sediments, **7**: 96–100; https://doi.org/10.1065/jss2007.02.208

Rożek, D., Nadłonek, W., Cabała, J., 2015. Forms of heavy metals (Zn, Pb, Cd) occurring in rhizospheres from the areas of former and contemporary Zn-Pb ore mining. Mining Science, **22**: 125–138.

Sobanska, S., Ricq, N., Laboudigue, A., Guillermo, R., Brémard, C., Laureyns, J., Merlin, J.C., Wignacourt, J.P., 1999. Microchemical investigations of dust emitted by a lead smelter. Environmental Science & Technology, **33**: 1334–1339; https://doi.org/10.1021/es9805270

Sobanska, S., Deneele, D., Barbillat, J., Ledesert, B., 2016. Natural weathering of slags from primary Pb-Zn smelting as evidenced by Raman microspectroscopy. Applied Geochemistry, **64**: 107–117; https://doi.org/10.1016/j.apgeochem.2015.09.011

Soto-Jiménez, M.F., Flegal, A.R., 2011. Childhood lead poisoning from the smelter in Torreón, México. Environmental Research, **111**: 590–596; https://doi.org/10.1016/j.envres.2011.01.020

Soto-Jiménez, M.F., Roos-Muñoz, S., Soto-Morales, S., Gómez-Lizarrága, L.E., Bucio-Galindo, L., 2023. Environmental and health implications of Pb-bearing particles in settled urban dust from an arid city affected by Pb-Zn factory emissions. Scientific Reports, **13**, 21287; https://doi.org/10.1038/s41598-023-48593-5

Stafilov, T., Šajn, R., Pančevski, Z., Boev, B., Frontasyeva, M.V., Strelkova, L.P., 2010. Heavy metal contamination of topsoils around a lead and zinc smelter in the Republic of Macedonia. Journal of Hazardous Materials, **175**: 896–914; https://doi.org/10.1016/j.jhazmat.2009.10.094

Tessier, A., Campbell, P.G.C., Bisson, M., 1979. Sequential extraction procedure for speciation of particulate trace metals. Analytical Chemistry, 51: 844–851.

Tyszka, R., Kierczak, J., Pietranik, A., Ettler, V., Mihaljevič, M., 2014. Extensive weathering of zinc smelting slag in a heap in Upper Silesia (Poland): potential environmental risks posed by mechanical disturbance of slag deposits. Applied Geochemistry, **40**: 70–81; https://doi.org/10.1016/j.apgeochem.2013.10.010

Tyszka, R., Pietranik, A., Kierczak, J., Zieliński, G., Darling, J., 2018. Cadmium distribution in Pb-Zn slags from Upper Silesia, Poland: Implications for cadmium mobility from slag phases to the environment. Journal of Geochemical Exploration, **186**: 215–224; https://doi.org/10.1016/j.gexplo.2017.12.001

USGS, 2022. U.S. Geological Survey, Mineral Commodity Summaries, January 2022 Zinc Statistics and Information. https://pubs.usgs.gov/periodicals/mcs2022/mcs2022-zinc.pdf

Van Damme, A., Degryse, F., Smolders, E., Sarret, G., Dewit, J., Swennen, R., Manceau A., 2010. Zinc speciation in mining and smelter contaminated overbank sediments by EXAFS spectroscopy. Geochimica et Cosmochimica Acta, **74**: 3707–3720; https://doi.org/10.1016/j.gca.2010.03.032

Vanaecker, M., Courtin-Nomade, A., Bril, H., Lenaina, J.-F., 2014. Behavior of Zn-bearing phases in base metal slag from France and Poland: a mineralogical approach for environmental purposes. Journal of Geochemical Exploration, **136**: 1–13; https://doi.org/10.1016/j.gexplo.2013.09.001

Viets, J.G., Leach, D.L., Lichte, F.E., Hopkins, R.T., Gent, C.A., Powell, J.W., 1996. Paragenetic and minor- and trace-element studies of Mississippi Valley-type ore deposits of the Silesian-Cracow district, Poland. Prace Państwowego Instytutu Geologicznego, **154**: 51–71.

Warchulski, R., Gawęda, A., Kądziołka-Gaweł, M., Szopa, K., 2015. Composition and element mobilization in pyrometallurgical slags from the Orzeł Biały smelting plant in the Bytom--Piekary Śląskie area, Poland. Mineralogical Magazine, **79**: 459–483; https://doi.org/10.1180/minmag.2015.079.2.21

Xu, D.-M., Fu, R.-B., Wang, J.-X., An, B.-H., 2022. The geochemical behaviors of potentially toxic elements in a typical lead/zinc (Pb/Zn) smelter contaminated soil with quantitative mineralogical assessments. Journal of Hazardous Materials, **424,** 127127; https://doi.org/10.1016/j.jhazmat.2021.127127

Zhang, X., Yang, L., Li, Y., Li, H., Wang, W., Ye, B., 2012. Impacts of lead/zinc mining and smelting on the environment and human health in China. Environmental Monitoring and Assessment, **184**: 2261–2273; https://doi.org/10.1007/s10661-011-2115-6

Zhou, Y., Jiang, D., Ding, D., Wu, Y., Wei, J., Kong, L., Long, T., Fan, T., Deng, S., 2022. Ecological-health risks assessment and source apportionment of heavy metals in agricultural soils around a super-sized lead-zinc smelter with a long production history, in China. Environmental Pollution, **307**, 119487; https://doi.org/10.1016/j.envpol.2022.119487

APPENDIX 1

Element concentrations in top-soil from the Katowice-Szopienice industrial area

Sample	Top-soil in the area	Pb	Zn	Fe	Cd	Tl	Ag	As	Sb	Cu	Sn	Ba	Mg	Ca	S
		mg kg^{-1}											%		
SZ 13	Area 1. The area of the former Uthemann zinc smelter	5929	10000	36400	124	5.1	12.4	161.5	45.2	688.6	25.8	864	0.38	0.74	0.32
SZ 14		9177	10000	131300	492	6.2	20.5	280.6	30.9	775.8	26.0	168	0.42	0.72	1.32
SZ 15		1574	10000	20500	96	3.7	5.9	76.4	6.3	166.9	9.7	300	0.20	0.23	0.23
SZ 16		1470	10000	32000	81	1.9	3.7	77.7	14.5	275.5	10.8	211	0.21	1.54	0.10
SZ 17		946	10000	15500	51	3.0	3.6	46.4	6.6	135.0	13.8	374	0.22	0.54	0.15
SZ 18		230	931	11200	5	0.5	0.5	16.7	2.4	51.4	4.9	340	0.18	0.29	0.04
SZ 19		1085	10000	27700	55	3.6	4.1	138.1	7.9	169.4	28.8	825	0.61	1.27	0.26
SZ 20		2083	10000	20700	149	3.6	9.3	53.8	4.7	173.9	4.1	300	0.22	0.39	0.45
SZ 21		581	10000	31900	783	2.9	1.2	12.8	1.0	59.0	1.8	1031	0.67	1.71	0.15
SZ 28	Area 2. The area of the former Rolling Mill and the Bernhardi zinc smelter	2424	10000	25400	89	20.5	11.1	128.8	26.4	1959.5	43.8	334	0.39	1.56	0.08
SZ 29		5927	10000	51200	155	18.3	47.5	147.3	109.0	2248.5	105.4	356	1.82	4.86	0.16
SZ 30		5734	10000	135600	347	8.8	15.3	412.1	48.4	438.9	33.6	477	1.30	2.40	0.29
SZ 7	Area 3. Areas west of the former Uthemann zinc smelter	3483	10000	30400	90	2.5	7.8	372.6	22.8	10000.0	307.2	256	0.57	0.98	0.08
SZ 8		1802	10000	25800	80	1.8	4.8	221.3	9.0	1721.7	57.8	272	0.40	0.68	0.07
SZ 9		2365	10000	34200	52	1.6	5.9	425.5	5.1	223.2	7.3	292	0.58	0.92	0.04
SZ 10		3187	10000	42000	55	2.1	6.7	591.4	6.3	189.1	6.6	315	0.75	1.47	0.04
SZ 11		>10000	10000	59900	217	6.2	62.3	820.0	145.9	1792.3	117.3	581	0.58	1.04	0.30
SZ 12		>10000	10000	34300	142	5.3	28.0	385.6	71.9	932.7	51.8	363	0.43	0.97	0.22
SZ 22		7856	10000	79300	83	1.2	19.8	1153.5	7.3	621.5	20.7	138	0.73	2.53	1.43
SZ 23		484	10000	8400	41	0.9	2.1	46.2	3.6	3059.7	4.3	142	0.11	0.20	0.06
SZ 24		211	1277	11300	8	0.4	0.5	21.5	1.1	30.9	1.9	216	0.25	0.48	0.04
SZ 25		678	3468	14800	22	0.5	8.3	104.2	1.6	69.4	2.3	185	0.32	0.73	0.04
SZ 1	Area 4. Along the River Rawa, to the N and NE of the former Uthemann zinc smelter	515	3740	8300	33	1.7	1.4	27.9	2.9	41.6	3.1	210	0.09	0.16	0.04
SZ 2		322	4185	10500	30	0.9	1.7	10.5	2.7	79.3	4.0	233	0.13	0.32	0.06
SZ 3		978	7601	26800	47	1.5	3.2	47.8	7.2	163.5	10.8	425	0.47	0.78	0.10
SZ 4		555	3032	10200	31	1.4	1.9	18.2	3.8	89.0	4.9	259	0.10	0.16	0.05
SZ 31		235	1054	12300	11	1.3	1.1	15.0	4.4	59.9	5.3	214	0.16	0.42	0.05
SZ 32		875	4056	20600	33	1.8	2.5	30.2	9.1	115.9	9.2	449	0.20	1.00	0.09
SZ 33		1793	6399	23600	44	5.0	3.1	153.3	9.2	57.3	5.5	307	1.23	2.87	0.53
SZ 34		59	305	7100	3	0.4	0.1	5.3	0.7	11.0	0.9	162	0.09	0.27	0.04
SZ 35		582	1857	14200	20	1.1	1.1	28.2	6.8	50.3	6.3	330	0.25	0.92	0.06
SZ 40		1458	3763	21400	32	5.9	7.1	171.6	17.0	91.5	9.4	318	0.33	0.95	0.05
SZ 5	Area 5. Urban square areas and childrens' playgrounds	252	2320	11000	25	1.1	1.0	24.7	5.0	68.3	12.4	191	0.11	0.65	0.06
SZ 6		431	2188	17800	22	2.4	1.1	58.0	2.8	80.8	4.7	257	0.14	0.33	0.04
SZ 26		2323	6129	25200	52	3.6	11.6	65.8	35.5	234.4	18.6	373	0.49	1.21	0.11
SZ 27		2022	3566	19700	35	2.0	8.9	49.5	32.7	190.9	20.4	347	0.31	0.69	0.10
SZ 36		683	1415	13300	11	0.7	1.6	31.0	6.0	57.6	6.1	306	0.16	0.39	0.05
SZ 37		2533	4504	19100	46	2.4	6.2	47.3	21.0	128.7	16.2	459	0.23	0.63	0.10
SZ 38		438	1748	15100	14	0.7	1.1	27.8	4.0	40.4	6.2	297	0.17	0.58	0.04
SZ 39		498	446	16700	4	0.9	1.0	33.0	25.5	36.8	12.0	323	0.11	0.16	0.04

APPENDIX 2

Summary of the Tessier et al. (1979) sequential extraction procedure

Step	Fractions	Reagent	Shaking time and temperature
1	Exchangeable (F1)	8 ml of 1 M $MgCl_2$ (pH 7) in 1 g soil	2 h at 25˚C
2	Bound to carbonates (F2)	8 ml of NaOAc (pH 5.0 with HOAc)	5 h at 25˚C
3	Amorphous iron-manganese oxides (F3)	20 ml of 0.04 M hydroxylamine hydrochloride in 25% acetic acid (pH 2 with HNO_3)	6 h at 96˚C
4	Organic-bound (F4)	5 ml of 30% H_2O_2 (pH 2), plus 3 ml of 0.02 M HNO_3 and 3 ml of 30% H_2O_2 (pH 2) Cool, add 20 ml of a mixture of 3.2 M NH_4Ac and 20% HNO_3	2 h at 85˚C
5	Residual (F5)	The residual fraction was digested by 8 ml of a mixture of HCl and 0.5 M HNO_3 Volume ratio of 3 to 1	30 min at 25˚C